



universität  
wien

# MASTERARBEIT

## Effective interaction in microgels

angestrebter akademischer Grad

Master of Science  
(MSc)

Verfasser:	Clemens Hanel
Studienkennzahl:	A 066 876
Studienrichtung:	Physik
Betreuer:	Univ.-Prof. Dipl.-Ing. Dr. Christos Likos

Wien, am 1. August 2013



# Abstract

Using a one component reduction formalism, we calculate the effective interaction and the counterion density profile for a microgel consisting of multilayered shell macroions. We follow a strategy that involves second order perturbation theory and obtain analytical expressions for the effective interactions by modelling the layers of the particles as linear combinations of homogeneously charged spheres. Furthermore, we apply the general result to the important case of core-shell microgels and compare the theory to the well known result for a microgel consisting of homogeneously charged, spherical macroions.



*Science is the great antidote to the poison of enthusiasm and superstition.*

Adam Smith



## Acknowledgements

Finally, with this master thesis in the field of soft matter physics, after a long interruption due to my extensive excursion into mathematics, I am completing my physics curriculum. I would like to thank my family and friends for their enduring support and patience, my supervisor Christos Likos for his commitment and for giving me the opportunity to enter—from my perspective—a completely new and interesting field of science, and finally, Peter Poier, Ronald Blaak, and Evelina Erlacher for fruitful input to my work.





# Contents

<b>Abstract</b>	<b>i</b>
<b>Acknowledgements</b>	<b>v</b>
<b>1. Introduction</b>	<b>1</b>
<b>2. Mathematical Framework</b>	<b>3</b>
2.1. Distributions . . . . .	3
2.2. Fourier transform . . . . .	4
2.3. Distributions and integrable regulators . . . . .	6
<b>3. Microgel model and theory</b>	<b>9</b>
3.1. Model . . . . .	9
3.2. Theory . . . . .	9
<b>4. Interaction for homogeneous macroions</b>	<b>19</b>
4.1. Electrostatic macroion interaction . . . . .	19
4.2. Effective interaction of microgel macroions . . . . .	25
<b>5. Interaction in multilayered-shell microgels</b>	<b>35</b>
5.1. Interaction of multilayered macroions . . . . .	36
5.2. Interaction of a layered macroion and a point charge . . . . .	40
5.3. Counterion density and effective interaction . . . . .	40
<b>6. Application to core-shell microgels</b>	<b>45</b>
<b>A. Fourier integral evaluation</b>	<b>55</b>
<b>Index</b>	<b>59</b>
<b>References</b>	<b>63</b>
<b>Curriculum Vitae</b>	<b>67</b>



# 1. Introduction

The notion of a *microgel* originates from a publication by William O. Baker from 1949 [Bak49]. In this article Baker described cross-linked polybutadiene latex particles. By cross-linking we refer to chemical bonds that link polymer chains to each other. In this context, when speaking of a *gel*, we consider the property of such materials to swell when added to an organic solvent, whereas *micro* points out the relatively small diameter of the gel particles, which is about 1  $\mu\text{m}$  or less. These microgel particles considered by Baker consist of a polymer network with high molecular weight and are therefore viewed as single, very large molecules. Nowadays, we describe microgels as *colloidal suspension* of gel particles, i. e. the individual particles are considered to be very large compared to the atomic scale but rather small compared to the macroscopic level, and they are dispersed in a solvent. The typical range of particles representing such a microgel is about 10 nm to 1000 nm. Dispersion of microgel particles in a solvent causes them to swell. Contrary to Baker's original suggestion gel particles can be formed not only by a single molecule but also by polyelectrolyte complex formation. In that case the individual particles consist of a number of shorter polymer chains, cf. [FuSa49, Mic65, FPLC07]. One of the most important properties of microgels is that their swelling is reversible and can depend on a lot of external parameters such as the pH value of the solvent, the temperature or the salt concentration. This also allows to tune the pair interaction between gel particles from hard-sphere-like interactions in the collapsed state to soft repulsions when expanded. However, the swelling does not affect the connectivity within the polymer network, whose stability originates mostly in strong covalent bonding forces.

In recent years the field of ionic microgels received a considerable amount of attention in theoretical approaches [SaVi99, SeRi99] as well as in applications [JeGu02, MFea03, MuSn95]. This field draws its motivation mainly from various applications in industry and medicine. An important application is, e.g. drug delivery methods where one is interested in using microgels to encapsulate and release pharmaceuticals in a controlled way, i. e. through change of an external parameter [MFea03, CHS05]. Further applications of microgels include sensor technology [RLL03, GSK05], photonic crystals [XKea03, LSea04] and purification technology [BTH03]. Important examples of ionic microgels in-

clude copolymers—that are polymers consisting of two monomeric constituents—made of *N*-isopropylacrylamide (NIPAM) or *N*-vinylcaprolactam (VCL) and an ionizable monomer such as acrylic acid [BRV05, ImFo11].

In this thesis we study the electrostatic interactions of core-shell microgels. When considering a particle of an ionic microgel the internal structure of such a *macroion* is dependent on the strength of the cross-linking. Weak cross-linking usually results in a fairly homogeneous distribution of the polymer chain and therefore in this case we consider the macroions to be homogeneously charged. However, increasing the strength of the cross-linking causes the polymer chains to rearrange in a way that resembles a core-shell structure [ARF13]. That is, the charge density of the macroion changes with respect to the distance from the macroions centre. In principle, such an ionic microgel solution is a multi-component-mixture of macroions, counterions, and ions of the electrolyte solvent. Since a full analytical treatment in terms of pair interactions in such a multi-body system is generally quite a keen challenge, the preferred approach is to treat the system at the level of *effective* interactions: By tracing out all degrees of freedom up to a single component, one obtains an equivalent one-component-system of so called *pseudoparticles* subject to an effective interaction. Previous work on this topic has already been carried out by A. Denton for the case of colloidal suspensions of non-penetrable charged macroions in [Den99] as well as for the case of solutions of star polymers and homogeneously charged microgel particles in [Den03]. The aim of this work is to extend the results of Denton to ionic solutions of core-shell macroions. Therefore, we largely follow the approach presented in [Den03] and employ second order perturbation theory to derive the counterion density profile and the effective interaction between macroions. For simplicity we restrict ourselves to a model where we ignore the electrostatic influence of the solvent ions and just consider a two component system of macroions and counterions. Furthermore, we assume that the macroions are completely penetrable by macroions as well as counterions and that the external parameters are known and fixed, so is the internal structure of the macroions.

The thesis is organized in the following way: In Chapter 2, we give a short introduction to the mathematical framework needed. Then, in Chapter 3, we describe the microgel model used in the remainder of the thesis and present the theoretical approach to calculate effective interactions via linear response theory. Afterwards, in Chapter 4, we recapitulate the case of homogeneously charged microgel particles in detail, and Chapter 5 is dedicated to the results for multilayered-shell microgels. Finally, in Chapter 6, we apply the previously obtained results to so called *core-shell* macroions.

## 2. Mathematical Framework

In this chapter we will give a short overview on the mathematical concepts used within the remainder of this work. Apart from basic analytic techniques, we mostly rely on distribution theory to extend the concept of functions, see [Fri98] for a more comprehensive introduction into this topic. The use of distributions allows us to employ the full power of Fourier transforms.

### 2.1. Distributions

As introduced by Laurent Schwartz in [Sch45], we view distributions as continuous linear functionals acting on some suitable function space. Since in this work we will extensively make use of Fourier transforms, we choose the *Schwartz space*  $\mathcal{S}(\mathbb{R}^n)$  as underlying function space to define the *tempered distributions*.

**2.1.1. DEFINITION (Schwartz space):** A smooth function  $\varphi$  on  $\mathbb{R}^n$  is considered to be an element of the Schwartz space  $\mathcal{S}(\mathbb{R}^n)$  if for all multiindices  $\alpha, \beta \in \mathbb{N}_0^n$  we have

$$\sup_{x \in \mathbb{R}^n} |x^\alpha \partial^\beta \varphi(x)| < \infty.$$

Here  $x^\alpha$  denotes the product  $\prod_{i=1}^n x_i^{\alpha_i}$ , similarly we proceed with  $\partial^\beta$ . This allows us to define the tempered distributions as topological dual space of the Schwartz space  $\mathcal{S}(\mathbb{R}^n)$ .

**2.1.2. DEFINITION (Tempered distributions):** We call a continuous linear functional  $u : \mathcal{S}(\mathbb{R}^n) \rightarrow \mathbb{R}$  a *tempered distribution* and denote the space of such  $u$  by  $\mathcal{S}'(\mathbb{R}^n)$ .

We write  $\varphi \mapsto \langle u, \varphi \rangle$  for the action of a distribution  $u$  on a function  $\varphi$  or, more frequently, by slight abuse of notation

$$\langle u, \varphi \rangle = \int_{\mathbb{R}^n} u(x) \varphi(x) \, d^n x.$$

## 2. Mathematical Framework

---

For obvious reasons such a functional  $u$  is continuous if and only if there exists a constant  $C \geq 0$  and an integer  $N \geq 0$  such that

$$|\langle u, \varphi \rangle| \leq C \sum_{|\alpha|, |\beta| \leq N} \sup |x^\alpha \partial^\beta \varphi| \text{ for all } \varphi \in \mathcal{S}(\mathbb{R}^n).$$

Examples of such distributions are the Dirac-delta distribution  $\delta$  defined on the real line by  $\langle \delta, \varphi \rangle := \varphi(0)$  or the Heaviside function

$$\Theta(x) = \begin{cases} 0 & \text{for } x < 0, \\ 1 & \text{for } x \geq 0. \end{cases}$$

Differentiation of distributions is defined in the following way: For a distribution  $u$  the derivative  $\partial^\alpha u$  is the distribution that satisfies the identity

$$\langle \partial^\alpha u, \varphi \rangle = (-1)^{|\alpha|} \langle u, \partial^\alpha \varphi \rangle. \quad (2.1)$$

Consider the following example, that shows a relation between the Heaviside function and the Dirac-delta distribution

**2.1.3. EXAMPLE:** We calculate the derivative of  $\Theta$ . By Equation (2.1) we have

$$\begin{aligned} \langle \Theta', \varphi \rangle &= -\langle \Theta, \varphi' \rangle = -\int_{-\infty}^{\infty} \Theta(x) \varphi'(x) dx \\ &= -\int_0^{\infty} \varphi'(x) dx = -\lim_{t \rightarrow \infty} \varphi(x) \Big|_{x=0}^t. \end{aligned}$$

Since  $\varphi \in \mathcal{S}(\mathbb{R})$ , we have  $\lim_{t \rightarrow \infty} \varphi(t) = 0$  and thus  $\langle \Theta', \varphi \rangle = \varphi(0)$ . Therefore we proved  $\Theta' = \delta$  in the sense of distributions.

## 2.2. Fourier transform

A large part of the calculations within the following chapters will be done in Fourier space. Hence, we will recapitulate the basic definitions and relations concerning Fourier transforms in this section. A detailed introduction to this topic can be found in [Fri98]. To

begin with, we give the definition of the Fourier transform of a function in the Schwartz space.

**2.2.1. DEFINITION:** We define the *Fourier transform* of a function  $\varphi$  in some suitable functions space on  $\mathbb{R}^b$ , such as the Schwartz space  $\mathcal{S}(\mathbb{R}^n)$ , as

$$\mathcal{F}_\varphi(\mathbf{k}) = \hat{\varphi}(\mathbf{k}) := \int_{\mathbb{R}^n} \varphi(\mathbf{x}) e^{-i\mathbf{k}\mathbf{x}} d^3x. \quad (2.2)$$

Note that in case  $\varphi \in \mathcal{S}(\mathbb{R}^n)$ , so is  $\hat{\varphi}$ . Then one can prove that the inverse transform exists and for a function  $\varphi$  reads

$$\mathcal{F}_\varphi^{-1}(\mathbf{x}) = \check{\varphi}(\mathbf{x}) := \frac{1}{(2\pi)^n} \int_{\mathbb{R}^n} \varphi(\mathbf{k}) e^{i\mathbf{k}\mathbf{x}} d^3k.$$

We may extend the Fourier transform (2.2) to a tempered distribution  $u \in \mathcal{S}'(\mathbb{R}^n)$  by the formula

$$\int_{\mathbb{R}^n} \hat{u}(\mathbf{k}) \varphi(\mathbf{k}) d^3k := \int_{\mathbb{R}^n} u(\mathbf{x}) \hat{\varphi}(\mathbf{x}) d^3x, \quad (2.3)$$

for all test functions  $\varphi \in \mathcal{S}(\mathbb{R}^n)$ .

**2.2.2. EXAMPLE:** We calculate the Fourier transform of  $\delta(\mathbf{x})$  on  $\mathbb{R}^n$ :

$$\begin{aligned} \int_{\mathbb{R}^n} \hat{\delta}(\mathbf{k}) \varphi(\mathbf{k}) d^n k &= \int_{\mathbb{R}^n} \delta(\mathbf{x}) \hat{\varphi}(\mathbf{x}) d^n x = \int_{\mathbb{R}^{2n}} \delta(\mathbf{x}) \varphi(\mathbf{k}) e^{-i\mathbf{k}\mathbf{x}} d^n k d^n x \\ &= \int_{\mathbb{R}^n} \varphi(\mathbf{k}) \int_{\mathbb{R}^n} \delta(\mathbf{x}) e^{-i\mathbf{k}\mathbf{x}} d^n x d^n k = \int_{\mathbb{R}^n} \mathbf{1}_{\mathbb{R}^n} \varphi(\mathbf{k}) d^n k. \end{aligned}$$

Hence, we have that  $\hat{\delta} = \mathbf{1}_{\mathbb{R}^n}$ .

Now consider a function  $\varphi$  on an  $n$ -cube with edge-length  $L$  and  $n$ -volume  $V$ , then we have

$$\hat{\varphi}(\mathbf{k}) = \int_V \varphi(\mathbf{x}) e^{-i\mathbf{k}\mathbf{x}} d^n x$$

and we may represent the function  $\varphi$  by its Fourier series

$$\varphi(\mathbf{x}) = \frac{1}{(2\pi)^n} \sum_{\mathbf{k}} e^{i\mathbf{k}\mathbf{x}} \hat{\varphi}(\mathbf{k}) (\Delta k)^n = \frac{1}{V} \sum_{\mathbf{k}} e^{i\mathbf{k}\mathbf{x}} \hat{\varphi}(\mathbf{k}),$$

where  $\Delta k = \frac{2\pi}{L}$ .

## 2. Mathematical Framework

---

Since in our treatment of effective interactions in a large part we deal with spherically symmetric functions, we also give the following representation of the Fourier transform for spherically symmetric functions, which is based on the Fourier-Sine transform. Now let  $\mathbf{r} \mapsto f(\mathbf{r})$  be such a spherically symmetric function on  $\mathbb{R}^3$ . Without loss of generality, we choose  $\mathbf{k}$  parallel to the  $z$ -axis of the coordinate system and obtain

$$\hat{f}(\mathbf{k}) = \int_{\mathbb{R}^3} f(r) e^{-i\mathbf{k}\mathbf{r}} d^3r = \int_0^{2\pi} \int_0^\infty \int_0^\pi f(r) e^{-ikr \cos \vartheta} r^2 \sin \vartheta d\vartheta dr d\varphi.$$

We substitute  $z := -\cos \vartheta$  and thus obtain, where obviously  $f(\mathbf{k}) = f(k)$ ,

$$\begin{aligned} \hat{f}(k) &= 2\pi \int_0^\infty r^2 f(r) \int_{-1}^1 e^{ikrz} dz dr = 4\pi \int_0^\infty r^2 f(r) \left( \frac{e^{ikr} - e^{-ikr}}{2ikr} \right) dr \\ &= \frac{4\pi}{k} \int_0^\infty r f(r) \sin(kr) dr. \end{aligned} \tag{2.4}$$

Similarly, the inverse Fourier transform for spherically symmetric functions reads

$$\check{f}(r) = \frac{1}{(2\pi)^2} \frac{2}{r} \int_0^\infty k f(k) \sin(kr) dk.$$

### 2.3. Distributions and integrable regulators

A technique of highly practical use is the Fourier transform of locally but not globally integrable functions via a sequence of convergence factors, called *integrable regulator*. Suppose we have a non-integrable function  $f$  and a continuous sequence of integrable functions  $(f_\lambda)_\lambda$  that converges pointwise to  $f$  for  $\lambda \rightarrow 0$ . Then one wishes to define

$$\hat{f}(\mathbf{k}) = \int_{\mathbb{R}^n} f(\mathbf{x}) e^{-i\mathbf{k}\mathbf{x}} d^n x := \lim_{\lambda \rightarrow 0} \int_{\mathbb{R}^n} f_\lambda(\mathbf{x}) e^{-i\mathbf{k}\mathbf{x}} d^n x.$$

When  $f$  is viewed as a *regular distribution*, i. e. we use that  $L^1_{\text{loc}}(\mathbb{R}^n) \subseteq \mathcal{S}'(\mathbb{R}^n)$ , this definition may be used in the following sense: Let  $\varphi$  be any Schwartz function on  $\mathbb{R}^n$  and let  $f_\lambda \in L^1(\mathbb{R}^n) \subseteq \mathcal{S}'(\mathbb{R}^n)$  such that  $\lim_{\lambda \rightarrow 0} f_\lambda = f$  and  $|f_\lambda| \leq |f|$  pointwise. Using Equation (2.3), we evaluate

$$\begin{aligned} \lim_{\lambda \rightarrow 0} \iint_{\mathbb{R}^{2n}} f_\lambda(\mathbf{x}) e^{-i\mathbf{k}\mathbf{x}} \varphi(\mathbf{k}) d^n x d^n k &= \lim_{\lambda \rightarrow 0} \iint_{\mathbb{R}^{2n}} f_\lambda(\mathbf{x}) e^{-i\mathbf{k}\mathbf{x}} \varphi(\mathbf{k}) d^n k d^n x \\ &= \lim_{\lambda \rightarrow 0} \int_{\mathbb{R}^n} f_\lambda(\mathbf{x}) \hat{\varphi}(\mathbf{x}) d^n x. \end{aligned} \tag{2.5}$$



Now, we want to apply the *dominated convergence theorem*, which allows us to commute integration and limit.

**2.3.1. THEOREM (Dominated convergence):** *If for some function  $h$  on  $\mathbb{R}^n$ , there exists a continuous sequence  $(h_\lambda)_\lambda$  or measurable functions that converges to  $h$  pointwise for  $\lambda \rightarrow 0$  and there also exists an integrable dominating function  $g(x)$  with  $|h_\lambda(x)| < g(x)$  for all  $x \in \mathbb{R}^n$  and  $\lambda > 0$ , then*

$$\lim_{\lambda \rightarrow 0} \int_{\mathbb{R}^n} h_\lambda(x) dx = \int_{\mathbb{R}^n} h(x) d^n x.$$

We choose  $h_\lambda(x) = f_\lambda(x)\hat{\phi}(x)$ ,  $h(x) = f(x)\hat{\phi}(x)$  and  $g(x) = |f(x)\hat{\phi}(x)|$ , thus

$$\lim_{\lambda \rightarrow 0} \int_{\mathbb{R}^n} f_\lambda(x)\hat{\phi}(x) d^n x = \int_{\mathbb{R}^n} \lim_{\lambda \rightarrow 0} f_\lambda(x)\hat{\phi}(x) d^n x = \int_{\mathbb{R}^n} f(x)\hat{\phi}(x) d^n x = \int_{\mathbb{R}^n} \hat{f}(k)\varphi(k) d^n k \quad (2.6)$$

and therefore combining (2.5) and (2.6) we obtain

$$\hat{f}(k) = \lim_{\lambda \rightarrow 0} \int_{\mathbb{R}^n} f_\lambda(x)e^{-ikx} d^n x \quad (2.7)$$

in the sense of distributions. As an illustration consider the following example, which we will also use frequently throughout the remainder of this work.

**2.3.2. EXAMPLE:** We want to calculate the Fourier transform of  $f(r) = \frac{1}{r}$  on  $\mathbb{R}^3$ . Therefore, we choose  $f_\lambda(r) = \frac{\exp(-\lambda r)}{r}$ . By Equation (2.7), we have

$$\hat{f}(k) = \lim_{\lambda \rightarrow 0} \int_{\mathbb{R}^3} \frac{e^{-\lambda r}}{r} e^{-ikr} d^3 r$$

Application of Equation (2.4) yields, using integration by parts,

$$\begin{aligned} \hat{f}(k) &= \frac{4\pi}{k} \lim_{\lambda \rightarrow 0} \int_0^\infty e^{-\lambda r} \sin(kr) dr = \frac{4\pi}{k} \lim_{\lambda \rightarrow 0} \frac{k}{\lambda} \int_0^\infty e^{-\lambda r} \cos(kr) dr \\ &= \frac{4\pi}{k} \lim_{\lambda \rightarrow 0} \left( \frac{k}{\lambda^2} - \frac{k^2}{\lambda^2} \int_0^\infty e^{-\lambda r} \sin(kr) dr \right). \end{aligned}$$

Hence

$$\frac{4\pi}{k} \lim_{\lambda \rightarrow 0} \left( 1 + \frac{k^2}{\lambda^2} \right) \int_0^\infty e^{-\lambda r} \sin(kr) dr = \frac{4\pi}{\lambda^2}$$

## 2. Mathematical Framework

---

and so with  $1 + \frac{k^2}{\lambda^2} = \frac{\lambda^2 + k^2}{\lambda^2}$

$$\hat{f}(k) = \lim_{\lambda \rightarrow 0} \frac{4\pi}{\lambda^2 + k^2}. \quad (2.8)$$

Thus, for  $k \neq 0$  we have  $\hat{f}(k) = \frac{4\pi}{k^2}$ .

## 3. Microgel model and theory

### 3.1. Model

We consider the following model of our microgel solution, based on the theory of ionic liquids that can be found in [HaMc06]: The system contains a number  $N_m$  of spherical macroions with radius  $a$ , mass  $M$  and over-all charge  $Ze$  and a number  $N_c$  of point-like counterions of charge  $ze$  and mass  $m$ . Here the number  $e$  denotes the elementary charge. The macroions and counterions are dispersed in an electrolyte solvent contained in some volume  $V$  with volume constant  $\varepsilon$  and temperature  $T$ . In general, we assume the electrolyte solvent to contain the same amount of positively and negatively charged microions, which all have the same valence  $|z|$  but in this presentation for reasons of simplicity, we ignore the effect of those salt ions.

Since we consider our microgel solution to be globally of neutral charge, it is a requirement that  $Zn_m + zn_c = 0$ , where  $n_m = \frac{N_m}{V}$  resp.  $n_c = \frac{N_c}{V}$  are the average macroion and counterion densities. Thus it follows that the macroion charge  $Z$  and the counterion charge  $z$  are of opposite sign. We may assume that there are three regions, where counterions can be observed: Free counterions outside the macroions, counterions within the macroions but sufficiently far away from the polymer chains and counterions surrounding the polymer chains. In our model we simply consider the counterions in the latter region to renormalize the effective charge of the macroion. Note that at this point we do not consider the internal structure of the macroions, i.e. we do not decide whether we have a homogeneously charged particle or a core-shell particle at hand. Changing the internal structure of the macroions purely results in different pair interactions, which we will treat in Chapters 4 and 5.

### 3.2. Theory

The goal of this section is to describe the one-component reduction and the linear response approximation for our model microgel solution. A suitable approach, which we

intend to follow, can be found in [Den99, Den00, Den03]. In the first paragraph, we mainly focus on the one-component reduction, in the remainder of the section we apply perturbation theory and derive the equations needed to obtain the approximate counterion density profile and approximate effective interaction taking linear response into account.

#### One-component reduction

Therefore, at first we consider the Hamiltonian of our microgel solution. We denote by  $\mathbf{R}_i, \mathbf{P}_i$  and  $\mathbf{r}_i, \mathbf{p}_i$  the coordinates as well as the momenta of the macroions and counterions, respectively. The Hamiltonian consists of three terms: the macroion energy, the counterion energy, and an interaction term

$$H(\mathbf{R}_i, \mathbf{r}_j, \mathbf{P}_i, \mathbf{p}_j) = H_m(\mathbf{R}_i, \mathbf{P}_i) + H_c(\mathbf{r}_j, \mathbf{p}_j) + H_{mc}(\mathbf{R}_i, \mathbf{r}_j, \mathbf{P}_i, \mathbf{p}_j). \quad (3.1)$$

Let us analyse these expressions in detail. The first term represents the kinetic and potential energy of a gas of macroions and therefore only depends on the macroion coordinates, thus

$$\begin{aligned} H_m(\mathbf{R}_i, \mathbf{P}_i) &= K_m(\mathbf{P}_i) + V_m(\mathbf{R}_i) \\ &= \frac{1}{2M} \sum_{i=1}^{N_m} \mathbf{P}_i^2 + \sum_{i=1}^{N_m} \sum_{j=1}^{i-1} v_{mm}(|\mathbf{R}_i - \mathbf{R}_j|). \end{aligned}$$

Here the expression  $v_{mm}(r)$  constitutes the bare pair potential of two macroions separated by a distance  $r$ . The actual form of  $v_{mm}$  depends on the internal configuration of the macroion and will be calculated in Chapter 4 for the case of a homogeneously charged macroion and in Chapter 5 for a multilayered particle. In a similar way, the second term in Equation (3.1)

$$\begin{aligned} H_c(\mathbf{r}_i, \mathbf{p}_i) &= K_c(\mathbf{p}_i) + V_c(\mathbf{r}_i) \\ &= \frac{1}{2m} \sum_{i=1}^{N_c} \mathbf{p}_i^2 + \sum_{i=1}^{N_c} \sum_{j=1}^{i-1} v_{cc}(|\mathbf{r}_i - \mathbf{r}_j|). \end{aligned}$$

consists of kinetic and potential energy for the counterions, where  $v_{cc}(r)$  is just the Coulomb pair potential for two point particles separated at a distance  $r$ , i. e.

$$v_{cc}(r) = \frac{1}{\epsilon} \frac{z^2 e^2}{r}.$$

The final term in Equation (3.1), however, constitutes the electrostatic interaction between macro- and counterions and reads

$$H_{\text{mc}} = \sum_{i=1}^{N_m} \sum_{j=1}^{N_c} v_{\text{mc}}(|\mathbf{R}_i - \mathbf{r}_j|) \quad (3.2)$$

$$= \iint \varrho_m(\mathbf{R}) \varrho_c(\mathbf{r}) v_{\text{mc}}(|\mathbf{R} - \mathbf{r}|) d^3r d^3R \quad (3.3)$$

with  $v_{\text{mc}}(r)$  being the macroion-counterion pair interaction. We denote by

$$\varrho_m(\mathbf{R}) = \sum_{i=1}^{N_m} \delta(\mathbf{R} - \mathbf{R}_i) \quad \varrho_c(\mathbf{r}) = \sum_{i=1}^{N_c} \delta(\mathbf{r} - \mathbf{r}_i) \quad (3.4)$$

the number densities of macroions and counterions, respectively. Here, the pair interaction  $v_{\text{mc}}$  again depends on the internal configuration of the macroions and we will give a detailed description in Chapters 4 and 5.

We aim at reducing the two-component mixture, consisting of macroions and counterions, to an equivalent one-component system governed by an effective Hamiltonian  $H_{\text{eff}}(\mathbf{R}_i, \mathbf{P}_i)$ , which only depends on the macroions coordinates. This can be achieved by tracing out the counterion degrees of freedom. Since we study a model microgel solution at a fixed temperature  $T$ , we find ourselves in a situation for which a treatment within the canonical ensemble is preferable. Therefore, we consider the canonical partition function derived from the microgel Hamiltonian, i. e. with  $\beta = \frac{1}{k_B T}$  we have

$$\mathcal{Z}(\beta, V) = \text{tr}_m \left( \text{tr}_c \left( e^{-\beta H(\mathbf{R}_i, \mathbf{P}_i, \mathbf{r}_j, \mathbf{p}_j)} \right) \right),$$

where

$$\text{tr}_c(f) = \frac{1}{h^{3N_c} N_c!} \iint_{V^{N_c} \times \mathbb{R}^{3N_c}} f(\mathbf{r}_i^\alpha, \mathbf{p}_i^\alpha) d^{3N_c} p d^{3N_c} r.$$

Factorizing the microgel Hamiltonian, we obtain the expression

$$\begin{aligned} \mathcal{Z}(\beta, V) &= \frac{1}{h^{3(N_m+N_c)} N_m! N_c!} \iint_{\mathbb{R}^{3(N_m+N_c)}} e^{-\beta(K_m+K_c)} d^{3N_m} P d^{3N_c} p \\ &\quad \iint_{V^{N_m+N_c}} e^{-\beta(V_m+V_c+H_{\text{mc}})} d^{3N_m} R d^{3N_c} r \\ &= \frac{1}{\Lambda_m^{3N_m} \Lambda_c^{3N_c} N_m! N_c!} \iint_{V^{N_m+N_c}} e^{-\beta(V_m+V_c+H_{\text{mc}})} d^{3N_m} R d^{3N_c} r, \end{aligned}$$

where  $\Lambda_m = \sqrt{\frac{2\pi\hbar\beta}{M}}$  and  $\Lambda_c = \sqrt{\frac{2\pi\hbar^2\beta}{m}}$  denote the thermal de Broglie wavelengths of the macroions and microions, respectively. The idea behind the reduction to a one-component system is to carry out the integration over the microion coordinates and write

### 3. Microgel model and theory

the canonical partition function as an integral over  $e^{-\beta H_{\text{eff}}}$  with respect to the macroion coordinates, where  $H_{\text{eff}} = H_m + F_c$  and  $F_c$  can be interpreted as the *free energy* of a non-uniform gas of counterions interacting with an external field generated by the macroions at positions  $\mathbf{R}_i$ . Thus, we write, separating the counterion degrees of freedom from the macroion ones,

$$\begin{aligned}\mathcal{Z}(\beta, V) &= \frac{1}{\Lambda_m^{3N_m} N_m!} \int_{V^{N_m}} e^{-\beta V_m} \int_{V^{N_c}} \frac{1}{\Lambda_c^{3N_c} N_c!} e^{-\beta(V_c + H_{mc})} d^{3N_c} r d^{3N_m} R \\ &= \frac{1}{\Lambda_m^{3N_m} N_m!} \int_{V^{N_m}} e^{-\beta V_m + \ln \left( \int_{V^{N_c}} \frac{1}{\Lambda_c^{3N_c} N_c!} \exp(-\beta(V_c + H_{mc})) d^{3N_c} r \right)} d^{3N_m} R \\ &= \frac{1}{\Lambda_m^{3N_m} N_m!} \int_{V^{N_m}} e^{-\beta V_m + \ln \tilde{\mathcal{Z}}} d^{3N_m} R,\end{aligned}$$

where  $\tilde{\mathcal{Z}}(\beta, V, \mathbf{R}_i) = \int_{V^{N_c}} \frac{1}{\Lambda_c^{3N_c} N_c!} e^{-\beta(V_c + H_{mc})} d^{3N_c} r$ . Defining the counterion free energy by  $F_c(\beta, V, \mathbf{R}_i) = -\frac{1}{\beta} \ln \tilde{\mathcal{Z}}(\beta, V, \mathbf{R}_i)$ , we obtain

$$\mathcal{Z}(\beta, V) = \frac{1}{\Lambda_m^{3N_m} N_m!} \int_{V^{N_m}} e^{-\beta(V_m + F_c)} d^{3N_m} R.$$

Since, when taking the thermodynamic limit, i. e. we let  $N_m, N_c, V \rightarrow \infty$  such that  $n_m, n_c$  are constant, we have to take into account divergences related to the long-ranged Coulomb interaction, we introduce a uniform compensating background energy  $E_b$  with a charge equally to that of the macroions. We therefore modify the counterion interaction such that  $V_c' = V_c + E_b$  and that  $H_{mc}' = H_{mc} - E_b$ , formally cancelling the infinities of each part of the Hamiltonian in the thermodynamic limit. Using charge neutrality  $Zn_m = -zn_c$ , the background energy  $E_b$  is given by (cf. [AsSt78])

$$\begin{aligned}E_b &= \frac{1}{2} n_c^2 \int_V \int_V \frac{z^2 e^2}{\epsilon |\mathbf{r} - \mathbf{r}'|} d^3 r d^3 r' + n_c \sum_{i=1}^{N_m} \int_V \frac{Z z e^2}{\epsilon |\mathbf{r} - \mathbf{R}_i|} d^3 r \\ &= \frac{1}{2} n_c^2 \int_V \int_V \frac{z^2 e^2}{\epsilon |\mathbf{r} - \mathbf{r}'|} d^3 r d^3 r' - \frac{n_c^2}{n_m} \sum_{i=1}^{N_m} \int_V \frac{z^2 e^2}{\epsilon |\mathbf{r} - \mathbf{R}_i|} d^3 r.\end{aligned}$$

In the thermodynamic limit we obtain

$$\begin{aligned}E_b &= \frac{1}{2} n_c^2 \iint_{\mathbb{R}^6} \frac{z^2 e^2}{\epsilon r} d^3 r d^3 r' - \frac{n_c^2}{n_m} \sum_{i=1}^{N_m} \int_{\mathbb{R}^3} \frac{z^2 e^2}{\epsilon r} d^3 r \\ &= \frac{1}{2} N_c n_c \int_{\mathbb{R}^3} \frac{z^2 e^2}{\epsilon r} d^3 r - \frac{n_c^2}{n_m} N_m \int_{\mathbb{R}^3} \frac{z^2 e^2}{\epsilon r} d^3 r \\ &= -\frac{1}{2} N_c n_c \int_{\mathbb{R}^3} v_{cc}(r) d^3 r.\end{aligned}$$

We want express the last integral in terms of the Fourier transform of  $v_{cc}(r)$ . Introducing an integrable regulator, we therefore consider

$$\int_{\mathbb{R}^3} v_{cc}(r) d^3r = \frac{z^2 e^2}{\varepsilon} \lim_{\lambda \rightarrow 0} \lim_{k \rightarrow 0} \int_0^\infty \frac{e^{\lambda r}}{r} e^{-ikr} d^3r.$$

We replace the expression on the right hand side according to Equation (2.8) and obtain

$$\int_{\mathbb{R}^3} v_{cc}(r) d^3r = \frac{z^2 e^2}{\varepsilon} \lim_{\lambda \rightarrow 0} \lim_{k \rightarrow 0} \frac{4\pi}{\lambda^2 + k^2} = \lim_{k \rightarrow 0} \hat{v}_{cc}(k)$$

and finally, we have

$$E_b = -\frac{1}{2} N_c n_c \lim_{k \rightarrow 0} \hat{v}_{cc}(k).$$

We now rewrite the free energy in terms of  $H_c'$  and  $H_{mc}'$  (omitting the macroion coordinates) as

$$F_c(\beta, V) = -\frac{1}{\beta} \ln \left[ \int_{V^{N_c}} \frac{1}{\Lambda_c^{3N_c} N_c!} e^{-\beta(V_c' + H_{mc}')} d^{3N_c} r \right], \quad (3.5)$$

where  $V_c'$  can be interpreted as the interaction of a classical one-component plasma, subject to a uniform compensating background, in the presence of neutral penetrable macroions.

### Approximation by linear response theory

This paragraph is dedicated to the perturbation theory approximation of the free energy, which later will allow us to calculate the counterion density profile and the effective interaction in second order. As a point of reference, we look at the free energy (3.5) and regard the macroion-counterion interaction as a perturbation of the counterion Hamiltonian, that is  $H_c(\lambda) = K_c + V_c' + H_{mc}'(\lambda)$ . Thus, the free energy of a one component plasma of counterions perturbed by some external interaction  $H_{mc}'(\lambda)$  is

$$F_c(\beta, V, \lambda) = -\frac{1}{\beta} \ln \left[ \int_{V^{N_c}} \frac{1}{\Lambda_c^{3N_c} N_c!} e^{-\beta(V_c' + H_{mc}'(\lambda))} d^{3N_c} r \right] =: -\frac{1}{\beta} \ln \tilde{Z}(\beta, V, \lambda).$$

Differentiating  $F_c$  with respect to  $\lambda$  gives

$$\begin{aligned} \frac{\partial}{\partial \lambda} F_c(\beta, V, \lambda) &= -\frac{1}{\beta \tilde{Z}(\beta, V, \lambda)} \frac{\partial}{\partial \lambda} \tilde{Z}(\beta, V, \lambda) \\ &= \frac{1}{\tilde{Z}(\beta, V, \lambda)} \int_{V^{N_c}} \frac{1}{\Lambda_c^{3N_c} N_c!} e^{-\beta(V_c' + H_{mc}'(\lambda))} \frac{\partial}{\partial \lambda} H_{mc}'(\lambda) d^{3N_c} r \\ &= \left\langle \frac{\partial}{\partial \lambda} H_{mc}'(\lambda) \right\rangle_\lambda, \end{aligned} \quad (3.6)$$

### 3. Microgel model and theory

---

where  $\langle \cdot \rangle_\lambda$  denotes an ensemble average governed by the canonical partition function  $\tilde{Z}(\beta, V, \lambda)$ . More precisely,

$$\langle f(\mathbf{r}_i) \rangle_\lambda = \frac{1}{\Lambda_c^{3N_c} N_c! \cdot \tilde{Z}(\beta, V, \lambda)} \int_{V^{N_c}} e^{-\beta(V_c' + H_{mc}'(\lambda))} f(\mathbf{r}_i) d^{3N_c} \mathbf{r}.$$

By integration of Equation (3.6) with respect to  $\lambda$ , we obtain the free energy in terms of  $\left\langle \frac{\partial}{\partial \lambda} H_{mc}'(\lambda) \right\rangle_\lambda$ . Hence,

$$F_c(\beta, V) = F_{\text{OCP}} + \int_0^1 \left\langle \frac{\partial}{\partial \lambda} H_{mc}'(\lambda) \right\rangle_\lambda d\lambda. \quad (3.7)$$

Here  $F_{\text{OCP}}$  denotes the free energy of a one-component plasma of counterions, i. e.

$$F_{\text{OCP}} = -\frac{1}{\beta} \ln \left[ \int_{V^{N_c}} \frac{1}{\Lambda_c^{3N_c} N_c!} e^{-\beta V_c'} d^{3N_c} \mathbf{r} \right]$$

Let us now consider the following situation: We take a one component-plasma of counterions in the presence of neutral macroions and start to charge adiabatically from zero to full charge. By  $\lambda$  we denote the fraction of the full charge. Partially charged macroions correspond to a setting, where  $H_{mc}(\lambda) = \lambda H_{mc}$  with  $\lambda \in [0, 1]$ . As a motivation consider the following closer look on the interaction between macroions and microions: The interaction is governed by the pair potential  $v_{mc}$  between a macroion at the origin and a counterion with charge  $q$  at distance  $\mathbf{r}$  which can be calculated from on the macroion charge density  $\varrho$  as

$$v_{mc}(r) = \frac{q}{\varepsilon} \int_{\mathbb{R}^6} \frac{\varrho(|\mathbf{x}|) \delta(\mathbf{y} - \mathbf{r})}{|\mathbf{x} - \mathbf{y}|} d^3x d^3y.$$

Partially charging the macroion means replacing  $\varrho(\mathbf{x})$  by  $\lambda \varrho(\mathbf{x})$ , thus the pair interaction of a partially charged macroion with a counterion reads

$$\frac{q}{\varepsilon} \int_{\mathbb{R}^6} \frac{\lambda \varrho(|\mathbf{x}|) \delta(\mathbf{y} - \mathbf{r})}{|\mathbf{x} - \mathbf{y}|} d^3x d^3y = \lambda v_{mc}(r).$$

So Equation (3.7) now reads, with  $E_b$  properly scaled

$$F_c(\beta, V) = F_{\text{OCP}} + \int_0^1 \langle H_{mc}' \rangle_\lambda d\lambda. \quad (3.8)$$

Recall Equation 3.2, we may write  $v_{mc}$  in terms of the inverse Fourier transform

$$\sum_{i=1}^{N_m} \sum_{j=1}^{N_c} v_{mc}(|\mathbf{R}_i - \mathbf{r}_j|) = \frac{1}{(2\pi)^3} \sum_{i=1}^{N_m} \sum_{j=1}^{N_c} \int e^{ik(\mathbf{R}_i - \mathbf{r}_j)} \hat{v}_{mc}(k) d^3k.$$



Since we are working in a finite volume  $V$ , the integration corresponds to a sum over discrete values of  $\mathbf{k}$ , so we have

$$\begin{aligned} \sum_{i=1}^{N_m} \sum_{j=1}^{N_c} v_{mc}(|\mathbf{R}_i - \mathbf{r}_j|) &= \frac{1}{V} \sum_{\mathbf{k} \neq 0} \sum_{i=1}^{N_m} \sum_{j=1}^{N_c} e^{i\mathbf{k}(\mathbf{R}_i - \mathbf{r}_j)} \hat{v}_{mc}(\mathbf{k}) + \frac{1}{V} \lim_{k \rightarrow 0} \sum_{i=1}^{N_m} \sum_{j=1}^{N_c} e^{i\mathbf{k}(\mathbf{R}_i - \mathbf{r}_j)} \hat{v}_{mc}(\mathbf{k}) \\ &= \frac{1}{V} \sum_{\mathbf{k} \neq 0} \left( \sum_{i=1}^{N_m} e^{i\mathbf{k}\mathbf{R}_i} \right) \left( \sum_{j=1}^{N_c} e^{-i\mathbf{k}\mathbf{r}_j} \right) \hat{v}_{mc}(\mathbf{k}) \\ &\quad + \frac{1}{V} \lim_{k \rightarrow 0} \left( \sum_{i=1}^{N_m} e^{i\mathbf{k}\mathbf{R}_i} \right) \left( \sum_{j=1}^{N_c} e^{-i\mathbf{k}\mathbf{r}_j} \right) \hat{v}_{mc}(\mathbf{k}) \end{aligned}$$

We insert the Fourier transforms of Equation (3.4) into the last equation and evaluate the the limit  $k \rightarrow 0$ . The summation terms obviously amount in the particle numbers for macroions and counterions. Summarized, this yields

$$\sum_{i=1}^{N_m} \sum_{j=1}^{N_c} v_{mc}(|\mathbf{R}_i - \mathbf{r}_j|) = \frac{1}{V} \sum_{\mathbf{k} \neq 0} \hat{q}_m(-\mathbf{k}) \hat{q}_c(\mathbf{k}) \hat{v}_{mc}(\mathbf{k}) + \lim_{k \rightarrow 0} N_m n_c \hat{v}_{mc}(\mathbf{k}).$$

Hence, we obtain for the ensemble average of the interaction term

$$\langle H_{mc}' \rangle_\lambda = \frac{1}{V} \sum_{\mathbf{k} \neq 0} \hat{q}_m(-\mathbf{k}) \hat{v}_{mc}(\mathbf{k}) \langle \hat{q}_c(\mathbf{k}) \rangle_\lambda + \lim_{k \rightarrow 0} N_m n_c \hat{v}_{mc}(\mathbf{k}) - E_b. \quad (3.9)$$

Considering a linear response of the induced counterion density to the external macroion-counterion interaction, cf. [HaMc06, Chapter 10], we obtain for  $\mathbf{k} \neq 0$

$$\langle \hat{q}_c(\mathbf{k}) \rangle_\lambda = \lambda \chi(\mathbf{k}) \hat{v}_{mc}(\mathbf{k}) \hat{q}_m(\mathbf{k}), \quad (3.10)$$

where  $\chi(k) = -\beta n_c S(k)$  is the linear response function of a one-component plasma. As outlined in [HaMc06, Chapter 3] or [Den03] this linear response function is proportional to the *static structure factor*, which by the Ornstein-Zernike relation equals  $S(k) = \frac{1}{1 - n_c \hat{c}(k)}$ . Here,  $c(r) = -\beta v_{cc}(r)$  denotes the two-particle direct correlation function. If we define the Bjerrum length  $\lambda_B = \frac{\beta e^2}{\epsilon}$  and the inverse Debye screening length  $\kappa = \sqrt{4\pi n_c z^2 \lambda_B}$ , we obtain

$$\chi(k) = -\frac{\beta n_c}{1 + \frac{\kappa^2}{k^2}}.$$

Thus, combining Equations (3.8), (3.9), and (3.10), the counterion free energy reads

$$\begin{aligned} F_c(\beta, V) &= F_{\text{OCP}} \\ &\quad + \int_0^1 \left( \frac{1}{V} \sum_{\mathbf{k} \neq 0} \lambda \chi(k) [\hat{v}_{mc}(\mathbf{k})]^2 \hat{q}_m(-\mathbf{k}) \hat{q}_m(\mathbf{k}) + \lim_{k \rightarrow 0} N_m n_c \hat{v}_{mc}(\mathbf{k}) - E_b \right) d\lambda \\ &= F_{\text{OCP}} + \frac{1}{2V} \sum_{\mathbf{k} \neq 0} \chi(k) [\hat{v}_{mc}(\mathbf{k})]^2 \hat{q}_m(-\mathbf{k}) \hat{q}_m(\mathbf{k}) + \lim_{k \rightarrow 0} N_m n_c \hat{v}_{mc}(\mathbf{k}) - E_b. \end{aligned}$$

### 3. Microgel model and theory

---

For the effective Hamiltonian  $H_{\text{eff}} = H_{\text{m}} + F_{\text{c}}$ , we have

$$H_{\text{eff}} = K_{\text{m}} + \sum_{i=1}^{N_{\text{m}}} \sum_{j=1}^{i-1} v_{\text{mm}}(|\mathbf{R}_i - \mathbf{R}_j|) + \frac{1}{2V} \sum_{\mathbf{k} \neq 0} \chi(\mathbf{k}) [\hat{v}_{\text{mc}}(\mathbf{k})]^2 \hat{q}_{\text{m}}(-\mathbf{k}) \hat{q}_{\text{m}}(\mathbf{k}) \\ + F_{\text{OCP}} + \lim_{k \rightarrow 0} N_{\text{m}} n_{\text{c}} \hat{v}_{\text{mc}}(k) - E_{\text{b}}.$$

Defining the induced interaction  $\hat{v}_{\text{ind}}(k) = \chi(k) [\hat{v}_{\text{mc}}(k)]^2$ , we recast  $H_{\text{eff}}$  as

$$H_{\text{eff}} = K_{\text{m}} + \sum_{i=1}^{N_{\text{m}}} \sum_{j=1}^{i-1} v_{\text{mm}}(|\mathbf{R}_i - \mathbf{R}_j|) + \frac{1}{2V} \sum_{\mathbf{k} \neq 0} \hat{v}_{\text{ind}}(k) \hat{q}_{\text{m}}(-\mathbf{k}) \hat{q}_{\text{m}}(\mathbf{k}) \\ + F_{\text{OCP}} + \lim_{k \rightarrow 0} N_{\text{m}} n_{\text{c}} \hat{v}_{\text{mc}}(k) - E_{\text{b}}.$$

Let us look more closely on the macroion pair interaction in Fourier space. We write

$$\sum_{i=1}^{N_{\text{m}}} \sum_{j=1}^{i-1} v_{\text{mm}}(|\mathbf{R}_i - \mathbf{R}_j|) = \frac{1}{V} \sum_{\mathbf{k}} \sum_{i=1}^{N_{\text{m}}} \sum_{j=1}^{i-1} e^{i\mathbf{k}(\mathbf{R}_i - \mathbf{R}_j)} \hat{v}_{\text{mm}}(\mathbf{k}) \\ = \frac{1}{2V} \sum_{\mathbf{k}} \left( \sum_{i=1}^{N_{\text{m}}} e^{i\mathbf{k}\mathbf{R}_i} \right) \left( \sum_{j=1}^{N_{\text{m}}} e^{-i\mathbf{k}\mathbf{R}_j} \right) \hat{v}_{\text{mm}}(\mathbf{k}) \\ - \frac{1}{2V} \sum_{\mathbf{k}} \sum_{i=j=1}^{N_{\text{m}}} e^{i\mathbf{k}(\mathbf{R}_i - \mathbf{R}_j)} \hat{v}_{\text{mm}}(\mathbf{k}) \\ = \frac{1}{2V} \sum_{\mathbf{k}} v_{\text{mm}}(\mathbf{k}) [\varrho_{\text{m}}(\mathbf{k}) \varrho_{\text{m}}(-\mathbf{k}) - N_{\text{m}}].$$

So the effective Hamiltonian reads

$$H_{\text{eff}} = K_{\text{m}} + \frac{1}{2V} \sum_{\mathbf{k}} v_{\text{mm}}(\mathbf{k}) [\varrho_{\text{m}}(\mathbf{k}) \varrho_{\text{m}}(-\mathbf{k}) - N_{\text{m}}] \\ + \frac{1}{2V} \sum_{\mathbf{k} \neq 0} \hat{v}_{\text{ind}}(k) \hat{q}_{\text{m}}(-\mathbf{k}) \hat{q}_{\text{m}}(\mathbf{k}) \\ + F_{\text{OCP}} + \lim_{k \rightarrow 0} N_{\text{m}} n_{\text{c}} \hat{v}_{\text{mc}}(k) - E_{\text{b}}$$

Now, in Fourier space we introduce the effective interaction as  $\hat{v}_{\text{eff}} = \hat{v}_{\text{mm}} + \hat{v}_{\text{ind}}$ , therefore we obtain

$$H_{\text{eff}} = K_{\text{m}} + \frac{1}{2V} \sum_{\mathbf{k}} v_{\text{eff}}(\mathbf{k}) [\varrho_{\text{m}}(\mathbf{k}) \varrho_{\text{m}}(-\mathbf{k}) - N_{\text{m}}] \\ - \frac{1}{2V} \lim_{k \rightarrow 0} \hat{v}_{\text{ind}}(k) \hat{q}_{\text{m}}(-\mathbf{k}) \hat{q}_{\text{m}}(\mathbf{k}) \\ + \frac{N_{\text{m}}}{2V} \sum_{\mathbf{k} \neq 0} \hat{v}_{\text{ind}}(k) + \frac{N_{\text{m}}}{2V} \lim_{k \rightarrow 0} \hat{v}_{\text{ind}}(k) \\ + F_{\text{OCP}} + \lim_{k \rightarrow 0} N_{\text{m}} n_{\text{c}} \hat{v}_{\text{mc}}(k) - E_{\text{b}}.$$

Expressing the last equation again in terms of functions in real space yields

$$H_{\text{eff}} = K_m + \sum_{i=1}^{N_m} \sum_{j=1}^{i-1} \hat{v}_{\text{eff}}(|\mathbf{R}_i - \mathbf{R}_j|) + E_0,$$

where by  $E_0$  we denote the so called *volume energy*

$$\begin{aligned} E_0 &= F_{\text{OCP}} + \frac{N_m}{2V} \sum_{k \neq 0} \hat{v}_{\text{ind}}(k) + \frac{N_m}{2V} \lim_{k \rightarrow 0} \hat{v}_{\text{ind}}(k) \\ &\quad - \frac{1}{2V} \lim_{k \rightarrow 0} \hat{v}_{\text{ind}}(k) \hat{q}_m(-\mathbf{k}) \hat{q}_m(\mathbf{k}) \\ &\quad + \lim_{k \rightarrow 0} N_m n_c \hat{v}_{\text{mc}}(k) + \frac{1}{2} N_c n_c \lim_{k \rightarrow 0} \hat{v}_{\text{cc}}(k) \\ &= F_{\text{OCP}} + \frac{N_m}{2} \lim_{r \rightarrow 0} \frac{e^{i\mathbf{k}r}}{V} \left( \sum_{k \neq 0} \hat{v}_{\text{ind}}(k) + \lim_{k \rightarrow 0} \hat{v}_{\text{ind}}(k) \right) \\ &\quad + N_m \lim_{k \rightarrow 0} \left[ -\frac{1}{2} n_m \hat{v}_{\text{ind}}(k) + n_c \hat{v}_{\text{mc}}(k) + \frac{1}{2} \frac{N_c}{N_m} n_c \hat{v}_{\text{cc}}(k) \right] \end{aligned}$$

Finally, using Fourier inversion and the charge neutrality condition  $Zn_m + zn_c = 0$ , we write the volume energy as

$$E_0 = F_{\text{OCP}} + \frac{N_m}{2} \lim_{r \rightarrow 0} v_{\text{ind}}(r) + N_m \lim_{k \rightarrow 0} \left[ -\frac{1}{2} n_m \hat{v}_{\text{ind}}(k) + n_c \hat{v}_{\text{mc}}(k) - \frac{Z}{2z} n_c \hat{v}_{\text{cc}}(k) \right].$$

So far, we completed the one-component reduction and linear response approximation of our model microgel solution, and we are left with the task of explicitly calculating the counterion density profile  $\langle \varrho_c(r) \rangle$  and the effective interaction energy  $v_{\text{eff}}(r)$  around a single macroion placed at the coordinate origin. This will be done in the remaining chapters of this work.



## 4. Interaction for homogeneous macroions

### 4.1. Electrostatic macroion interaction

The interaction energy of two charge distributions on  $\mathbb{R}^3$  in a medium with electric permittivity  $\varepsilon$  reads (integrability assumed)

$$U = \frac{1}{\varepsilon} \int_{\mathbb{R}^6} \frac{\varrho_1(\mathbf{x})\varrho_2(\mathbf{y})}{|\mathbf{x} - \mathbf{y}|} d^3x d^3y. \quad (4.1)$$

In this chapter we assume the microgel macroions to be homogeneously charged spheres. Thus, let  $\varrho_1, \varrho_2$  be the charge distributions of two homogeneously charged spheres of radius  $a$ , both with charge  $Ze$  and separated by a distance  $\mathbf{r}$ . Thus, we may set  $\varrho_2(\mathbf{x}) = \varrho_1(\mathbf{x} - \mathbf{r})$  and choose  $\varrho_1(\mathbf{x}) = \frac{3Ze}{4\pi a^3} \Theta(a - |\mathbf{x}|) = \varrho_0 \cdot \Theta(a - |\mathbf{x}|)$ , where  $\Theta$  denotes the Heaviside function. Inserting this charge distribution into Equation (4.1), we obtain the macroion pair interaction as a function of the spheres' distance  $\mathbf{r}$

$$v_{\text{mm}}(\mathbf{r}) = \frac{\varrho_0^2}{\varepsilon} \int_{\mathbb{R}^6} \frac{\Theta(a - |\mathbf{x}|)\Theta(a - |\mathbf{y} - \mathbf{r}|)}{|\mathbf{x} - \mathbf{y}|} d^3x d^3y.$$

The electrostatic potential per unit of charge density subject to the source  $\varrho_1$  is given by

$$\Phi(\mathbf{y}) := \int_{\mathbb{R}^3} \frac{\Theta(a - |\mathbf{x}|)}{|\mathbf{x} - \mathbf{y}|} d^3x = \int_{B_a(0)} \frac{1}{|\mathbf{x} - \mathbf{y}|} d^3x = \int_0^{2\pi} \int_0^a \int_0^\pi \frac{x^2 \sin \vartheta}{|\mathbf{x} - \mathbf{y}|} d\vartheta dx d\varphi.$$

By employing spherical symmetry of the charge distribution, we may choose  $\mathbf{y}$  parallel to the  $z$ -axis of the coordinate system. Then, we obviously obtain the squared distance  $(\mathbf{x} - \mathbf{y})^2 = x^2 + y^2 - 2\mathbf{x} \cdot \mathbf{y} = x^2 + y^2 - 2xy \cos \vartheta$ , so the potential is

$$\Phi(\mathbf{y}) := 2\pi \int_0^a x^2 \int_0^\pi \frac{\sin \vartheta}{\sqrt{x^2 + y^2 - 2xy \cos \vartheta}} d\vartheta dx \quad (4.2)$$

#### 4. Interaction for homogeneous macroions

---

We substitute  $u := -\cos \vartheta$ , thus

$$\begin{aligned}\Phi(\mathbf{y}) &:= 2\pi \int_0^a x^2 \int_{-1}^1 \frac{1}{\sqrt{x^2 + y^2 + 2xyu}} du dx \\ &= 2\pi \int_0^a x^2 \left( \frac{1}{xy} (|x+y| - |x-y|) \right) dx\end{aligned}$$

since  $\int \frac{1}{\sqrt{ax+b}} = \frac{2}{a} \sqrt{ax+b} + C$ . We distinguish between the two cases  $y \leq x$  and  $y > x$ . In the first case we obtain the integrand  $2x$ , in the second case we obtain  $\frac{2x^2}{y}$ . Hence we have for  $y > a$

$$\Phi(\mathbf{y}) = 4\pi \int_0^a \frac{x^2}{y} dx = \frac{4\pi a^3}{3} \cdot \frac{1}{y},$$

and for  $y \leq a$

$$\Phi(\mathbf{y}) = 4\pi \left( \int_0^y \frac{x^2}{y} dx + \int_y^a x dx \right) = 4\pi \left( \frac{1}{3} y^2 + \frac{a^2}{2} - \frac{y^2}{2} \right) = 2\pi a^2 - \frac{2\pi}{3} y^2$$

Obviously,  $\Phi$  is a spherically symmetric function. Thus, altogether this yields

$$\Phi(y) = \frac{4\pi a^2}{3} \begin{cases} \frac{3}{2} - \frac{1}{2} \frac{y^2}{a^2} & \text{for } y \leq a, \\ \frac{a}{y} & \text{for } y > a, \end{cases} \quad (4.3a)$$

$$(4.3b)$$

or with  $\varrho_0 = \frac{3Ze}{4\pi a^3}$  inserted

$$\Phi(y) = \begin{cases} \frac{3Ze}{2a} - \frac{Ze}{2a^3} y^2 & \text{for } y \leq a, \\ \frac{Ze}{y} & \text{for } y > a. \end{cases} \quad (4.4a)$$

$$(4.4b)$$

Now, we have for the interaction energy

$$v_{\text{mm}}(\mathbf{r}) = \frac{\varrho_0^2}{\varepsilon} \int_{\mathbb{R}^3} \Phi(y) \Theta(a - |\mathbf{y} - \mathbf{r}|) d^3 y.$$

To calculate this energy, we substitute  $\mathbf{z} = \mathbf{y} - \mathbf{r}$  (which, since a translation, leaves the volume element invariant). This yields

$$v_{\text{mm}}(\mathbf{r}) = \frac{\varrho_0^2}{\varepsilon} \int_{\mathbb{R}^3} \Phi(|\mathbf{z} + \mathbf{r}|) \Theta(a - |\mathbf{z}|) d^3 z = \frac{\varrho_0^2}{\varepsilon} \int_{B_a(0)} \Phi(|\mathbf{z} + \mathbf{r}|) d^3 z.$$

As a matter of fact, in spherical coordinates we have

$$v_{\text{mm}}(\mathbf{r}) = \frac{q_0^2}{\varepsilon} \int_0^{2\pi} \int_0^a \int_0^\pi \Phi(|\mathbf{z} + \mathbf{r}|) z^2 \sin \vartheta \, d\vartheta \, dz \, d\varphi.$$

Again, we distinguish between different cases: In case  $r > 2a$  the distance  $|\mathbf{z} + \mathbf{r}| > a$  for  $\mathbf{z} \in B_a(0)$  and thus we have for the potential  $\Phi(|\mathbf{z} + \mathbf{r}|) = \frac{4\pi a^3}{3} \frac{1}{|\mathbf{z} + \mathbf{r}|}$ . Spherical symmetry allows us to choose  $\mathbf{r}$  parallel to the  $z$ -axis and therefore,

$$v_{\text{mm}}(\mathbf{r}) = \frac{8\pi^2 a^3 q_0^2}{3\varepsilon} \int_0^a z^2 \int_0^\pi \frac{\sin \vartheta}{\sqrt{z^2 + r^2 + 2rz \cos \vartheta}} \, d\vartheta \, dz.$$

Substitution analogously to Equation (4.2) gives

$$\begin{aligned} v_{\text{mm}}(\mathbf{r}) &= \frac{8\pi^2 a^3 q_0^2}{3\varepsilon} \int_0^a z^2 \int_{-1}^1 \frac{1}{\sqrt{z^2 + r^2 - 2rzu}} \, du \, dz \\ &= -\frac{8\pi^2 a^3 q_0^2}{3\varepsilon} \int_0^a z^2 \left( \frac{1}{zr} (|z - r| - |z + r|) \right) \, dz \\ &= \frac{8\pi^2 a^3 q_0^2}{3\varepsilon} \int_0^a z^2 \left( \frac{1}{zr} (|z + r| - |z - r|) \right) \, dz. \end{aligned}$$

Since  $r > 2a$  and  $z < a$ , we have  $r > z$  and therefore the integrand reads  $\frac{2z^2}{r}$ , so

$$v_{\text{mm}}(\mathbf{r}) = \frac{16\pi^2 a^3 q_0^2}{3\varepsilon r} \int_0^a z^2 \, dz = \frac{16\pi^2 a^6 q_0^2}{9\varepsilon r} \quad (4.5)$$

Again, using  $q_0 = \frac{3Ze}{4\pi a^3}$ , we obtain the (spherically symmetric) interaction energy

$$v_{\text{mm}}(r) = \frac{Z^2 e^2}{\varepsilon r}.$$

Now we turn to the cases  $a \leq r \leq 2a$  and  $r \leq a$ , which involve somewhat more considerations. Depending on the direction and length of  $\mathbf{r}$ , we have to consider the potential function  $\Phi(|\mathbf{z} + \mathbf{r}|)$  either for  $|\mathbf{z} + \mathbf{r}| \leq a$  or for  $|\mathbf{z} + \mathbf{r}| > a$ . Again, we choose  $\mathbf{r}$  to be parallel to the  $z$ -axis, then we have  $a^2 = |\mathbf{z} + \mathbf{r}|^2 = z^2 + r^2 + 2rz \cos \vartheta$ , thus a circle of radius  $z$  around the origin intersects the one of radius  $a$  around  $-\mathbf{r}$  at the angle  $\vartheta_0 = \arccos \frac{a^2 - z^2 - r^2}{2rz}$  for  $0 \leq \vartheta_0 \leq \pi$ .

Thus, we conclude that in case  $a \leq r$  for a given value of  $z \geq r - a$  we are outside  $B_a(-\mathbf{r})$  if  $0 \leq \vartheta < \arccos \frac{a^2 - z^2 - r^2}{2rz}$  and inside  $B_a(-\mathbf{r})$  if  $\arccos \frac{a^2 - z^2 - r^2}{2rz} \leq \vartheta \leq \pi$ . Setting

#### 4. Interaction for homogeneous macroions

---

$u := -\cos \theta$  this allows us to write down the interaction energy as a sum of three integrals to be specified below

$$\begin{aligned} v_{\text{mm}}(\mathbf{r}) &= \frac{q_0^2}{\varepsilon} \int_0^{2\pi} \int_0^a \int_0^\pi \Phi(|\mathbf{z} + \mathbf{r}|) z^2 \sin \vartheta \, d\vartheta \, dz \, d\varphi \\ &= I_1 + I_2 + I_3. \end{aligned}$$

The domains of integration for the integrals  $I_1$ ,  $I_2$ ,  $I_3$  are illustrated in Figure 4.1. Here,  $I_1$  denotes the integral over the ball  $B_{r-a}(0)$ , where  $\Phi$  is of the form (4.3b),  $I_2$  denotes the integral over the domain  $B_a(0) \setminus (B_{r-a}(0) \cup B_a(-\mathbf{r}))$ , where  $\Phi$  is also of the form (4.3b), and  $I_3$  denotes the integral over the domain  $B_a(0) \cap B_a(-\mathbf{r})$ , where  $\Phi$  is of the form (4.3a).

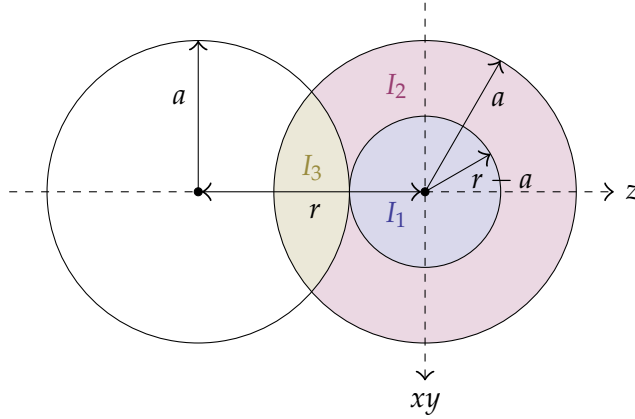


Figure 4.1: Domains of integration for  $I_1$ ,  $I_2$ , and  $I_3$

Since all occurring functions obey azimuthal symmetry, we obtain a factor  $2\pi$  for the  $\varphi$ -integration. We start calculating  $I_1$ , so

$$\begin{aligned} I_1 &= \frac{8\pi^2 a^3 q_0^2}{3\varepsilon} \int_0^{r-a} \int_{-1}^1 \frac{1}{\sqrt{z^2 + r^2 - 2rzu}} z^2 \, du \, dz \\ &= \frac{8\pi^2 a^3 q_0^2}{3\varepsilon} \int_0^{r-a} \frac{z^2}{rz} (|r+z| - |r-z|) \, dz. \end{aligned}$$



Now  $z \leq r - a \leq r$ , thus

$$I_1 = \frac{8\pi^2 a^3 \varrho_0^2}{3\epsilon} \int_0^{r-a} \frac{z}{r} (r + z - r + z) dz \quad (4.6a)$$

$$= \frac{8\pi^2 a^3 \varrho_0^2}{3\epsilon} \int_0^{r-a} \frac{2z^2}{r} dz \quad (4.6b)$$

$$= \frac{8\pi^2 a^3 \varrho_0^2}{3\epsilon} \cdot \left( 2a^2 - \frac{2a^3}{3r} - 2ar + \frac{2r^2}{3} \right). \quad (4.6c)$$

Similarly, we proceed for  $I_2$ , and we have

$$I_2 = \frac{8\pi^2 a^3 \varrho_0^2}{3\epsilon} \int_{r-a}^a \int_{-1}^{\frac{z^2+r^2-a^2}{2rz}} \frac{1}{\sqrt{z^2+r^2-2rzu}} z^2 du dz \quad (4.7a)$$

$$= \frac{8\pi^2 a^3 \varrho_0^2}{3\epsilon} \int_{r-a}^a \left( \frac{r+z}{rz} - \frac{a}{rz} \right) z^2 dz = \frac{8\pi^2 a^3 \varrho_0^2}{3\epsilon} \int_{r-a}^a \frac{z(r+z-a)}{r} dz \quad (4.7b)$$

$$= \frac{8\pi^2 a^3 \varrho_0^2}{3\epsilon} \left( -2a^2 + \frac{2a^3}{3r} + \frac{5ar}{2} - \frac{5r^2}{6} \right). \quad (4.7c)$$

Finally, we calculate  $I_3$

$$I_3 = \frac{8\pi^2 a^3 \varrho_0^2}{3\epsilon} \int_{r-a}^a \int_{\frac{z^2+r^2-a^2}{2rz}}^1 \left( \frac{3}{2a} - \frac{1}{2a^3} (z^2 + r^2 - 2rzu) \right) z^2 du dz \quad (4.8a)$$

$$= \frac{8\pi^2 a^3 \varrho_0^2}{3\epsilon} \int_{r-a}^a \left( \frac{5az}{8r} - \frac{3rz}{4a} + \frac{r^3 z}{8a^3} + \frac{3z^2}{2a} - \frac{r^2 z^2}{2a^3} - \frac{3z^3}{4ar} + \frac{3rz^3}{4a^3} - \frac{z^4}{2a^3} + \frac{z^5}{8a^3 r} \right) dz \quad (4.8b)$$

$$= \frac{8\pi^2 a^3 \varrho_0^2}{3\epsilon} \left( \frac{4a^2}{5} - \frac{ar}{2} - \frac{r^2}{6} + \frac{r^3}{8a} - \frac{r^5}{240a^3} \right). \quad (4.8c)$$

Summarized, this yields

$$\begin{aligned} v_{\text{mm}}(r) &= \frac{8\pi^2 a^3 \varrho_0^2}{3\epsilon} \left( \frac{4a^2}{5} - \frac{r^2}{3} + \frac{r^3}{8a} - \frac{r^5}{240a^3} \right) \\ &= \frac{Z^2 e^2}{\epsilon a} \left[ \frac{6}{5} - \frac{1}{2} \left( \frac{r}{a} \right)^2 + \frac{3}{16} \left( \frac{r}{a} \right)^3 - \frac{1}{160} \left( \frac{r}{a} \right)^5 \right]. \end{aligned} \quad (4.9)$$

The remaining case is  $r \leq a$ . We conclude that in this case, for a given value of  $z \geq a - r$ , we are outside  $B_a(-\mathbf{r})$  if  $0 \leq \vartheta < \arccos \frac{a^2 - z^2 - r^2}{2rz}$ , and we are inside  $B_a(-\mathbf{r})$  if  $\arccos \frac{a^2 - z^2 - r^2}{2rz} \leq \vartheta \leq \pi$ . Again, we set  $u := -\cos \theta$  and write down the interaction

#### 4. Interaction for homogeneous macroions

energy as a sum of three integrals  $U(\mathbf{r}) = J_1 + J_2 + J_3$ , whose domains of integration are illustrated in Figure 4.2.

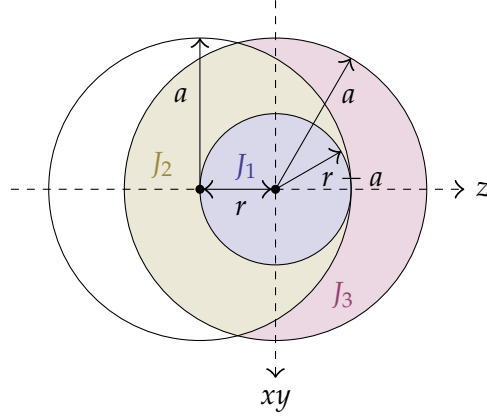


Figure 4.2: Domains of integration for  $J_1$ ,  $J_2$ , and  $J_3$

Here  $J_1$  denotes the integral over the ball  $B_{a-r}(0)$ , where  $\Phi$  takes the form (4.3a),  $J_2$  denotes the integral over  $(B_a(0) \cap B_a(-\mathbf{r})) \setminus B_{a-r}(0)$ , where  $\Phi$  is also of the form (4.3a), and  $J_3$  denotes the integral over  $B_a(0) \setminus B_a(-\mathbf{r})$ . Incorporating azimuthal symmetry again we have

$$\begin{aligned} J_1 &= \frac{8\pi^2 a^3 q_0^2}{3\epsilon} \int_0^{a-r} \int_{-1}^1 \left( \frac{3}{2a} - \frac{1}{2a^3} (z^2 + r^2 - 2rzu) \right) z^2 du dz \\ &= \frac{8\pi^2 a^3 q_0^2}{3\epsilon} \int_0^{a-r} \left( \frac{3z^2}{a} - \frac{r^2 z^2}{a^3} - \frac{z^4}{a^3} \right) dz \\ &= \frac{8\pi^2 a^3 q_0^2}{3\epsilon} \left( \frac{4a^2}{5} - 2ar + \frac{2r^2}{3} + \frac{2r^3}{a} - \frac{2r^4}{a^2} + \frac{8r^5}{15a^3} \right). \end{aligned}$$

We proceed for  $J_2$  in the same way, hence

$$\begin{aligned} J_2 &= \frac{8\pi^2 a^3 q_0^2}{3\epsilon} \int_{a-r}^a \int_{\frac{z^2+r^2-a^2}{2rz}}^1 \left( \frac{3}{2a} - \frac{1}{2a^3} (z^2 + r^2 - 2rzu) \right) z^2 du dz \\ &= \frac{8\pi^2 a^3 q_0^2}{3\epsilon} \int_{a-r}^a \left( \frac{5az}{8r} - \frac{3rz}{4a} + \frac{r^3 z}{8a^3} + \frac{3z^2}{2a} - \frac{r^2 z^2}{2a^3} - \frac{3z^3}{4ar} + \frac{3rz^3}{4a^3} - \frac{z^4}{2a^3} + \frac{z^5}{8a^3 r} \right) dz \\ &= \frac{8\pi^2 a^3 q_0^2}{3\epsilon} \left( \frac{3ar}{2} - \frac{5r^2}{6} - \frac{15r^3}{8a} + \frac{2r^4}{a^2} - \frac{43r^5}{80a^3} \right). \end{aligned}$$

Finally,  $J_3$  gives

$$\begin{aligned}
 J_3 &= \frac{8\pi^2 a^3 q_0^2}{3\epsilon} \int_{a-r}^a \int_{-1}^{\frac{z^2+r^2-a^2}{2rz}} \frac{1}{\sqrt{z^2+r^2-2rzu}} z^2 du dz \\
 &= \frac{8\pi^2 a^3 q_0^2}{3\epsilon} \int_{a-r}^a \left( \frac{r+z}{rz} - \frac{a}{rz} \right) z^2 dz = \frac{8\pi^2 a^3 q_0^2}{3\epsilon} \int_{a-r}^a \frac{z(r+z-a)}{r} dz \\
 &= \frac{8\pi^2 a^3 q_0^2}{3\epsilon} \left( \frac{a^2}{2} - \frac{a^3}{6r} - \frac{a^2}{2} + \frac{a^3}{6r} + \frac{ar}{2} - \frac{r^2}{6} \right) \\
 &= \frac{8\pi^2 a^3 q_0^2}{3\epsilon} \left( \frac{ar}{2} - \frac{r^2}{6} \right).
 \end{aligned}$$

Adding up the three integrals, we again obtain exactly (4.9)

$$\begin{aligned}
 v_{\text{mm}}(r) &= \frac{8\pi^2 a^3 q_0^2}{3\epsilon} \left( \frac{4a^2}{5} - \frac{r^2}{3} + \frac{r^3}{8a} - \frac{r^5}{240a^3} \right) \\
 &= \frac{Z^2 e^2}{\epsilon a} \left[ \frac{6}{5} - \frac{1}{2} \left( \frac{r}{a} \right)^2 + \frac{3}{16} \left( \frac{r}{a} \right)^3 - \frac{1}{160} \left( \frac{r}{a} \right)^5 \right].
 \end{aligned}$$

Hence, altogether this yields the interaction energy as an at least continuously differentiable function of  $r$ , which reads

$$v_{\text{mm}}(r) = \begin{cases} \frac{Z^2 e^2}{\epsilon a} \left[ \frac{6}{5} - \frac{1}{2} \left( \frac{r}{a} \right)^2 + \frac{3}{16} \left( \frac{r}{a} \right)^3 - \frac{1}{160} \left( \frac{r}{a} \right)^5 \right] & \text{for } 0 \leq r \leq 2a, \\ \frac{Z^2 e^2}{\epsilon r} & \text{for } 2a < r. \end{cases} \quad (4.10)$$

## 4.2. Effective interaction of microgel macroions

The bare Coulomb interaction energy between a macroion of charge  $Ze$  and a counterion of charge  $ze$  reads

$$v_{\text{mc}}(r) = \begin{cases} \frac{Zze^2}{2\epsilon a} \left( 3 - \frac{r^2}{a^2} \right) & \text{for } 0 \leq r \leq a, \\ \frac{Zze^2}{\epsilon r} & \text{for } a < r. \end{cases} \quad (4.11a)$$

$$\quad (4.11b)$$

We need the Fourier transform of  $v_{\text{mc}}$ , thus we calculate for  $k \neq 0$

$$\begin{aligned}
 \hat{v}_{\text{mc}} &= \frac{4\pi}{k} \int_0^\infty r v_{\text{mc}}(r) \sin(kr) dr \\
 &= \frac{4\pi}{k} \int_0^a \frac{Zze^2}{2\epsilon a} \left( 3r - \frac{r^3}{a^2} \right) \sin(kr) dr + \frac{4\pi}{k} \int_a^\infty \frac{Zze^2}{\epsilon} \sin(kr) dr
 \end{aligned}$$

#### 4. Interaction for homogeneous macroions

---

We split the integration into three additive terms, such that  $\hat{v}_{\text{mc}} = \frac{4\pi Zze^2}{k\epsilon}(I_1 + I_2 + I_3)$ . This yields

$$\begin{aligned} I_1 &= \frac{3}{2a} \int_0^a r \sin(kr) \, dr = \frac{3}{2a} \left( -\frac{a}{k} \cos(ka) + \frac{1}{k} \int_0^a \cos(kr) \, dr \right) \\ &= \frac{3}{2ka} \left( -a \cos(ka) + \frac{1}{k} \sin(ka) \right) \\ &= -\frac{3}{2k} \cos(ka) + \frac{3}{2k^2 a} \sin(ka), \end{aligned}$$

for  $I_2$  we obtain

$$\begin{aligned} I_2 &= -\frac{1}{2a^3} \int_0^a r^3 \sin(kr) \, dr = -\frac{1}{2a^3} \left( -\frac{a^3}{k} \cos(ka) + \frac{3}{k} \int_0^a r^2 \cos(kr) \, dr \right) \\ &= -\frac{1}{2ka^3} \left( -a^3 \cos(ka) + 3 \left( \frac{a^2}{k} \sin(ka) - \frac{2}{k} \int_0^a r \sin(kr) \, dr \right) \right) \\ &= -\frac{1}{2ka^3} \left( -a^3 \cos(ka) + \frac{3}{k} \left( a^2 \sin(ka) - 2 \left( -\frac{a}{k} \cos(ka) + \frac{1}{k} \int_0^a \cos(kr) \, dr \right) \right) \right) \\ &= -\frac{1}{2ka^3} \left( -a^3 \cos(ka) + \frac{3}{k} \left( a^2 \sin(ka) - \frac{2}{k} \left( -a \cos(ka) + \frac{1}{k} \sin(ka) \right) \right) \right) \\ &= \frac{1}{2k} \cos(ka) - \frac{3}{2k^2 a} \sin(ka) - \frac{3}{k^3 a^2} \cos(ka) + \frac{3}{k^4 a^3} \sin(ka), \end{aligned}$$

The third integral reads

$$I_3 = \int_a^\infty \sin(kr) \, dr,$$

which is obviously divergent. Let us consider the following modification

$$I_3 = \int_0^\infty \sin(kr) \, dr - \int_0^a \sin(kr) \, dr.$$

Introducing an integrable regulator, we obtain by Equation (2.8) that

$$\int_0^\infty \sin(kr) \, dr = \frac{k}{4\pi} \mathcal{F} \left( \frac{1}{r} \right) = \lim_{\lambda \rightarrow 0} \frac{k}{\lambda^2 + k^2} = \frac{1}{k}.$$

The second part of the integral we simply evaluate and hence, obtain

$$I_3 = \frac{1}{k} - \left( 1 - \frac{\cos(ka)}{k} \right) = \frac{\cos(ka)}{k}. \quad (4.12)$$

The sum of the three integrals yields

$$I_1 + I_2 + I_3 = -\frac{3}{k^3 a^2} \cos(ka) + \frac{3}{k^4 a^3} \sin(ka),$$

so, finally, for  $k \neq 0$

$$\hat{v}_{\text{mc}} = -\frac{12\pi Zze^2}{k^4 a^2 \epsilon} \left( \cos(ka) - \frac{\sin(ka)}{ka} \right).$$

We assume the macroions to be at positions  $\mathbf{R}_j$ , thus the macroion density equals

$$\varrho_{\text{m}}(\mathbf{k}) = \sum_{j=1}^{N_{\text{m}}} \delta(\mathbf{r} - \mathbf{R}_j),$$

where  $N_{\text{m}}$  is the total number of macroions. Obviously  $\hat{\varrho}_{\text{m}}(\mathbf{k}) = \sum_{j=1}^{N_{\text{m}}} e^{-i\mathbf{k}\mathbf{R}_j}$ .

Using the linear response approximation from Equation (3.10), we can calculate the counterion density around a single macroion at the coordinate origin, i. e.  $\varrho_{\text{m}}(\mathbf{r}) = \delta(\mathbf{r})$ , by

$$\langle \hat{\varrho}_{\text{c}}(\mathbf{k}) \rangle = \chi(k) \hat{v}_{\text{mc}}(k) \quad (4.13)$$

since  $\hat{\varrho}_{\text{m}}(\mathbf{k}) = 1$  and  $\chi(k) = -\frac{\epsilon \lambda_{\text{B}} n_{\text{c}}}{e^2 + \epsilon \lambda_{\text{B}} n_{\text{c}} \hat{v}_{\text{cc}}(k)}$  with  $v_{\text{cc}}(r)$  the bare Coulomb interaction between two counterions of distance  $r$  and charge  $ze$ . Here  $\lambda_{\text{B}} = \frac{\beta e^2}{\epsilon}$  denotes the Bjerrum length, i. e. the distance, where the Coulomb interaction is of comparable magnitude to the thermal energy. From Equation (2.8), we obtain  $\hat{v}_{\text{cc}}(k) = \frac{4\pi z^2 e^2}{\epsilon k^2}$  and so

$$\begin{aligned} \langle \hat{\varrho}_{\text{c}}(\mathbf{k}) \rangle &= \frac{\epsilon \lambda_{\text{B}} n_{\text{c}}}{e^2 + \frac{4\pi \lambda_{\text{B}} n_{\text{c}} z^2 e^2}{k^2}} \frac{12\pi Zze^2}{k^4 a^2 \epsilon} \left( \cos(ka) - \frac{\sin(ka)}{ka} \right) \\ &= \frac{12\pi Zz \lambda_{\text{B}} n_{\text{c}}}{(k^2 + 4\pi \lambda_{\text{B}} n_{\text{c}} z^2) k^2 a^2} \left( \cos(ka) - \frac{\sin(ka)}{ka} \right). \end{aligned} \quad (4.14)$$

Using the inverse Debye screening length  $\kappa := \sqrt{4\pi n_{\text{c}} z^2 \lambda_{\text{B}}}$ , Equation (4.14) reads

$$\langle \hat{\varrho}_{\text{c}}(\mathbf{k}) \rangle = \frac{Z}{z} \frac{3\kappa^2}{k^2 a^2 (k^2 + \kappa^2)} \left( \cos(ka) - \frac{\sin(ka)}{ka} \right).$$

Application of the inverse Fourier transform gives the counterion density profile as a function of the distance to the macroion. Hence, we calculate

$$\begin{aligned} \bar{\varrho}_{\text{c}}(r) &:= \langle \varrho_{\text{c}}(r) \rangle = \frac{1}{(2\pi)^2} \frac{2}{r} \int_0^\infty k \frac{Z}{z} \frac{3\kappa^2}{k^2 a^2 (k^2 + \kappa^2)} \left( \cos(ka) - \frac{\sin(ka)}{ka} \right) \sin(kr) dk \\ &= \frac{6Z\kappa^2}{4\pi^2 r a^2} \int_0^\infty \frac{\sin(kr)}{k(k^2 + \kappa^2)} \left( \cos(ka) - \frac{\sin(ka)}{ka} \right) dk. \end{aligned}$$

#### 4. Interaction for homogeneous macroions

---

We split this expression into two integrals such that  $\bar{q}_c(r) = \frac{6Z\kappa^2}{4\pi^2 rza^2}(I_1 - I_2)$ . Evaluating the first integral, we obtain

$$\begin{aligned} I_1 &= \int_0^\infty \frac{\sin(kr) \cos(ka)}{k(k^2 + \kappa^2)} dk \\ &= \frac{1}{2} \int_0^\infty \frac{\sin(k(r-a)) + \sin(k(r+a))}{k(k^2 + \kappa^2)} dk. \end{aligned} \quad (4.15)$$

Substitution with  $x := \frac{k}{\kappa}$  in Equation (4.15) and expansion into partial fractions gives

$$\begin{aligned} I_1 &= \frac{1}{2\kappa^2} \int_0^\infty \frac{\sin(x\kappa(r-a)) + \sin(x\kappa(r+a))}{x(x^2 + 1)} dx \\ &= \frac{1}{2\kappa^2} \int_0^\infty \left( \frac{\sin(x\kappa(r-a)) + \sin(x\kappa(r+a))}{x} - x \frac{\sin(x\kappa(r-a)) + \sin(x\kappa(r+a))}{x^2 + 1} \right) dx. \end{aligned}$$

It is a well known fact, that  $\int_0^\infty \frac{\sin(\lambda x)}{x} dx = \frac{\pi}{2} \operatorname{sgn} \lambda$  and  $\int_0^\infty \frac{x \sin(\lambda x)}{x^2 + 1} dx = \frac{\pi}{2} e^{-|\lambda|} \operatorname{sgn} \lambda$ . Hence, we consider for  $a, r$ , and  $\kappa > 0$

$$\int_0^\infty \frac{\sin(x\kappa(r \pm a))}{x} dx = \frac{\pi}{2} \operatorname{sgn}(r \pm a)$$

and

$$\int_0^\infty \frac{x \sin(x\kappa(r \pm a))}{x^2 + 1} dx = \frac{\pi}{2} e^{-\kappa|r \pm a|} \operatorname{sgn}(r \pm a).$$

Summarized, we have

$$I_1 = \frac{\pi}{4\kappa^2} (\operatorname{sgn}(r-a)(1 - e^{-\kappa|r-a|}) + (1 - e^{-\kappa(r+a)})). \quad (4.16)$$

Now, we proceed in a similar way for the second integral,

$$\begin{aligned} I_2 &= \int_0^\infty \frac{1}{k^2 a(k^2 + \kappa^2)} \sin(kr) \sin(ka) dk \\ &= \frac{1}{2a} \int_0^\infty \frac{\cos(k(r-a)) - \cos(k(r+a))}{k^2(k^2 + \kappa^2)} dk. \end{aligned}$$

Again, we substitute with  $x := \frac{k}{\kappa}$  and expand into partial fractions, which yields

$$\begin{aligned} I_2 &= \frac{1}{2a\kappa^3} \int_0^\infty \left( \frac{\cos(x\kappa(r-a)) - \cos(x\kappa(r+a))}{x^2(x^2+1)} \right) \\ &= \frac{1}{2a\kappa^3} \int_0^\infty \left( \frac{\cos(x\kappa(r-a)) - \cos(x\kappa(r+a))}{x^2} - \frac{\cos(x\kappa(r-a)) - \cos(x\kappa(r+a))}{x^2+1} \right) dx. \end{aligned} \quad (4.17)$$

Consider the first term in (4.17), through integration by parts

$$\int \frac{\cos(\lambda x)}{x^2} dx = -\frac{\cos(\lambda x)}{x} - \lambda \int \frac{\sin(\lambda x)}{x} dx$$

we obtain

$$\begin{aligned} \int_0^\infty \frac{\cos(x\kappa(r-a)) - \cos(x\kappa(r+a))}{x^2} dx &= -\lim_{\beta \rightarrow \infty} \lim_{\alpha \rightarrow 0} \frac{\cos(x\kappa(r-a)) - \cos(x\kappa(r+a))}{x} \Big|_\alpha^\beta \\ &\quad - \kappa(r-a) \int_0^\infty \frac{\sin(\kappa(r-a))}{x} dx \\ &\quad + \kappa(r+a) \int_0^\infty \frac{\sin(\kappa(r+a))}{x} dx \\ &= -\lim_{\beta \rightarrow \infty} \frac{\cos(\beta\kappa(r-a))}{\beta} + \lim_{\beta \rightarrow \infty} \frac{\cos(\beta\kappa(r+a))}{\beta} \\ &\quad + \lim_{\alpha \rightarrow 0} \frac{\cos(\alpha\kappa(r-a)) - \cos(\alpha\kappa(r+a))}{\alpha} \\ &\quad + \frac{\pi}{2} \kappa(r+a - |r-a|) \end{aligned}$$

Obviously, since the cosine is a bounded function, both the  $\beta$ -limits tend to zero. However, the  $\alpha$ -limits need some more consideration: Expansion into a power series at  $\alpha_0 = 0$  gives

$$\begin{aligned} \frac{\cos(\alpha\kappa(r-a)) - \cos(\alpha\kappa(r+a))}{\alpha} &= \frac{1}{\alpha} \sum_{n=0}^\infty (-1)^n \frac{\kappa^{2n}((r-a)^{2n} - (r+a)^{2n})}{(2n)!} \alpha^{2n} \\ &= \alpha \sum_{n=1}^\infty (-1)^n \frac{\kappa^{2n}((r-a)^{2n} - (r+a)^{2n})}{(2n)!} \alpha^{2n-2}, \end{aligned}$$

where the power series  $\sum_{n=1}^\infty (-1)^n \frac{\kappa^{2n}((r-a)^{2n} - (r+a)^{2n})}{(2n)!} \alpha^{2n-2}$  converges. Thus,

$$\lim_{\alpha \rightarrow 0} \frac{\cos(\alpha\kappa(r-a)) - \cos(\alpha\kappa(r+a))}{\alpha} = 0$$

#### 4. Interaction for homogeneous macroions

---

and

$$\int_0^\infty \frac{\cos(x\kappa(r-a)) - \cos(x\kappa(r+a))}{x^2} dx = \frac{\pi}{2}\kappa(r+a-|r-a|)$$

This leaves us calculating the second term in (4.17). We have

$$\int_0^\infty \frac{\cos(x\kappa(r-a)) - \cos(x\kappa(r+a))}{x^2 + 1} dx = \frac{\pi}{2}(e^{-\kappa|r-a|} - e^{-\kappa(r+a)})$$

since  $\int_0^\infty \frac{\cos(\lambda x)}{1+x^2} dx = \frac{\pi}{2}e^{-|\lambda|}$ . Summarized, we obtain

$$I_2 = \frac{\pi}{4\kappa^2} \left( \frac{1}{a}(r+a-|r-a|) - \frac{1}{\kappa a}(e^{-\kappa|r-a|} - e^{-\kappa(r+a)}) \right). \quad (4.18)$$

Finally, we combine the results of (4.16) and (4.18), so

$$\begin{aligned} \bar{q}_c(r) &= \frac{Z}{z} \frac{3}{8\pi r a^2} \left( \operatorname{sgn}(r-a)(1 - e^{-\kappa|r-a|}) + (1 - e^{-\kappa(r+a)}) \right. \\ &\quad \left. - \frac{1}{a}(r+a-|r-a|) + \frac{1}{\kappa a}(e^{-\kappa|r-a|} - e^{-\kappa(r+a)}) \right). \end{aligned}$$

On one hand in case  $r > a$  this yields

$$\begin{aligned} \bar{q}_c(r) &= \frac{Z}{z} \frac{3}{8\pi r a^2} \left( 1 - e^{-\kappa(r-a)} + 1 - e^{-\kappa(r+a)} - 2 + \frac{1}{\kappa a}(e^{-\kappa(r-a)} - e^{-\kappa(r+a)}) \right) \\ &= -\frac{Z}{z} \frac{3}{4\pi r a^2} \left( \frac{e^{-\kappa r}}{2}(e^{\kappa a} + e^{\kappa a}) - \frac{e^{-\kappa r}}{2\kappa a}(e^{\kappa a} - e^{-\kappa a}) \right) \\ &= -\frac{Z}{z} \frac{3}{4\pi r a^2} e^{-\kappa r} \left( \cosh(\kappa a) - \frac{\sinh(\kappa a)}{\kappa a} \right), \end{aligned}$$

on the other hand in case  $r < a$  we have

$$\begin{aligned} \bar{q}_c(r) &= \frac{Z}{z} \frac{3}{8\pi r a^2} \left( -1 + e^{-\kappa(a-r)} + 1 - e^{-\kappa(a+r)} - \frac{2r}{a} + \frac{1}{\kappa a}(e^{-\kappa(a-r)} - e^{-\kappa(a+r)}) \right) \\ &= -\frac{Z}{z} \frac{3}{4\pi r a^2} \left( -\frac{e^{-\kappa a}}{2}(e^{\kappa r} - e^{-\kappa r}) \right) + \frac{r}{a} - \frac{e^{-\kappa a}}{2\kappa a}(e^{\kappa r} - e^{-\kappa r}) \\ &= -\frac{Z}{z} \frac{3}{4\pi r a^2} \left( \frac{r}{a} - \left(1 + \frac{1}{\kappa a}\right) e^{-\kappa a} \sinh(\kappa r) \right). \end{aligned} \quad (4.19)$$

If  $r = a$ , we obtain

$$\begin{aligned} \bar{q}_c(r) &= \frac{Z}{z} \frac{3}{8\pi r a^2} \left( 1 - e^{-2\kappa a} - 2 + \frac{1}{\kappa a}(1 - e^{-2\kappa a}) \right) \\ &= -\frac{Z}{z} \frac{3}{8\pi r a^2} \left( 1 + e^{-2\kappa a} - \frac{1}{\kappa a} + \frac{e^{-2\kappa a}}{\kappa a} \right) \\ &= -\frac{Z}{z} \frac{3}{8\pi r a^2} \left( 1 - \frac{1}{\kappa a} + e^{-2\kappa a} \left( 1 + \frac{1}{\kappa a} \right) \right) \\ &= -\frac{Z}{z} \frac{3}{8\pi r a^2} \left( 1 - \frac{1}{\kappa a} + e^{-\kappa a}(e^{\kappa a} - 2\sinh(\kappa a)) \left( 1 + \frac{1}{\kappa a} \right) \right) \\ &= -\frac{Z}{z} \frac{3}{4\pi r a^2} \left( 1 - \left( 1 + \frac{1}{\kappa a} \right) e^{-\kappa a} \sinh(\kappa a) \right) \end{aligned}$$



which is exactly (4.19) for  $r = a$ . Therefore, the counterion density reads

$$\bar{\rho}_c(r) = -\frac{Z}{z} \frac{3}{4\pi a^2 r} \begin{cases} \frac{r}{a} - \left(1 + \frac{1}{\kappa a}\right) e^{-\kappa a} \sinh(\kappa r) & \text{for } r \leq a, \\ e^{-\kappa r} \left( \cosh(\kappa a) - \frac{\sinh(\kappa a)}{\kappa a} \right) & \text{for } r > a. \end{cases} \quad (4.20)$$

We obtain the counterion-induced interaction by

$$\begin{aligned} \hat{v}_{\text{ind}}(k) &= \chi(k) [\hat{v}_{\text{mc}}(k)]^2 = \langle \hat{\rho}_c(k) \rangle \hat{v}_{\text{mc}}(k) \\ &= -\frac{Z}{z} \frac{3\kappa^2}{k^2 a^2 (k^2 + \kappa^2)} \left( \cos(ka) - \frac{\sin(ka)}{\kappa a} \right) \frac{12\pi Z z e^2}{k^4 a^2 \varepsilon} \left( \cos(ka) - \frac{\sin(ka)}{\kappa a} \right) \\ &= -\frac{36\pi Z^2 e^2}{\varepsilon k^6 a^4} \frac{\kappa^2}{k^2 + \kappa^2} \left( \cos(ka) - \frac{\sin(ka)}{\kappa a} \right)^2. \end{aligned}$$

To calculate the effective interaction, we also have to take the macroion-macroion-interaction into account, so  $v_{\text{eff}} = v_{\text{ind}} + v_{\text{mm}}$  or in Fourier space  $\hat{v}_{\text{eff}} = \hat{v}_{\text{ind}} + \hat{v}_{\text{mm}}$ , respectively. Following the calculation of Section 4.1, by (4.10) we have

$$v_{\text{mm}}(r) = \begin{cases} \frac{Z^2 e^2}{\varepsilon a} \left[ \frac{6}{5} - \frac{1}{2} \left( \frac{r}{a} \right)^2 + \frac{3}{16} \left( \frac{r}{a} \right)^3 - \frac{1}{160} \left( \frac{r}{a} \right)^5 \right] & \text{for } 0 \leq r \leq 2a, \\ \frac{Z^2 e^2}{\varepsilon r} & \text{for } 2a < r. \end{cases}$$

Thus we calculate the Fourier transform of  $v_{\text{mm}}$ , i. e.

$$\begin{aligned} \hat{v}_{\text{mm}}(k) &= \frac{4\pi}{k} \int_0^\infty r v_{\text{mm}}(r) \sin(kr) dr \\ &= \frac{4\pi Z^2 e^2}{k\varepsilon} \int_0^{2a} \left[ \frac{6}{5} \frac{r}{a} - \frac{1}{2} \left( \frac{r}{a} \right)^3 + \frac{3}{16} \left( \frac{r}{a} \right)^4 - \frac{1}{160} \left( \frac{r}{a} \right)^6 \right] \sin(kr) dr \\ &\quad + \frac{4\pi Z^2 e^2}{k\varepsilon} \int_{2a}^\infty \sin(kr) dr \\ &= \frac{4\pi Z^2 e^2}{k\varepsilon} (I_1 + I_2). \end{aligned}$$

From (4.12) we immediately obtain  $I_2 = \frac{\cos(2ka)}{k}$ . The first integral  $I_1$  can be solved via the following iteration formulas based on integration by parts. We have

$$\begin{aligned} \int r^n \sin(kr) dr &= -\frac{r^n}{k} \cos(kr) + \frac{n}{k} \int r^{n-1} \cos(kr) dr, \\ \int r^n \cos(kr) dr &= \frac{r^n}{k} \sin(kr) - \frac{n}{k} \int r^{n-1} \sin(kr) dr. \end{aligned}$$

#### 4. Interaction for homogeneous macroions

---

Hence,  $I_1$  reads

$$I_1 = \frac{9}{2k^7 a^6} - \frac{9 \cos(2ka)}{2k^7 a^6} - \frac{9 \sin(2ka)}{k^6 a^5} + \frac{9}{2k^5 a^4} + \frac{9 \cos(2ka)}{2k^5 a^4} - \frac{\cos(2ka)}{k}.$$

Altogether, we have

$$\begin{aligned} \hat{v}_{\text{eff}}(k) &= \frac{36\pi Z^2 e^2}{\epsilon k^6 a^4} \left[ \frac{1}{2k^2 a^2} - \frac{\cos(2ka)}{2k^2 a^2} - \frac{\sin(2ka)}{ka} + \frac{\cos(2ka)}{2} + \frac{1}{2} \right. \\ &\quad \left. - \frac{\kappa^2}{k^2 + \kappa^2} \left( \cos(ka) - \frac{\sin(ka)}{ka} \right)^2 \right] \\ &= \frac{36\pi Z^2 e^2}{\epsilon k^6 a^4} \left[ \frac{1}{2k^2 a^2} - \frac{\cos^2(ka)}{2k^2 a^2} + \frac{\sin^2(ka)}{2k^2 a^2} - \frac{2 \sin(ka) \cos(ka)}{ka} \right. \\ &\quad \left. + \frac{\cos^2(ka)}{2} - \frac{\sin^2(ka)}{2} + \frac{1}{2} - \frac{\kappa^2}{k^2 + \kappa^2} \left( \cos(ka) - \frac{\sin(ka)}{ka} \right)^2 \right] \\ &= \frac{36\pi Z^2 e^2}{\epsilon k^6 a^4} \left[ \frac{1}{2k^2 a^2} - \frac{\cos^2(ka)}{2k^2 a^2} - \frac{\sin^2(ka)}{2k^2 a^2} - \frac{2 \sin(ka) \cos(ka)}{ka} - \frac{\cos^2(ka)}{2} \right. \\ &\quad \left. - \frac{\sin^2(ka)}{2} + \frac{1}{2} + \cos^2(ka) + \frac{\sin^2(ka)}{k^2 a^2} - \frac{\kappa^2}{k^2 + \kappa^2} \left( \cos(ka) - \frac{\sin(ka)}{ka} \right)^2 \right] \\ &= \frac{36\pi Z^2 e^2}{\epsilon k^6 a^4} \left[ -\frac{2 \sin(ka) \cos(ka)}{ka} + \cos^2(ka) + \frac{\sin^2(ka)}{k^2 a^2} \right. \\ &\quad \left. - \frac{\kappa^2}{k^2 + \kappa^2} \left( \cos(ka) - \frac{\sin(ka)}{ka} \right)^2 \right] \\ &= \frac{36\pi Z^2 e^2}{\epsilon k^6 a^4} \left[ \left( \cos(ka) - \frac{\sin(ka)}{ka} \right)^2 - \frac{\kappa^2}{k^2 + \kappa^2} \left( \cos(ka) - \frac{\sin(ka)}{ka} \right)^2 \right] \\ &= \frac{36\pi Z^2 e^2}{\epsilon k^4 a^4} \frac{1}{k^2 + \kappa^2} \left( \cos(ka) - \frac{\sin(ka)}{ka} \right)^2. \end{aligned}$$

One obtains the effective interaction via the inverse Fourier transform

$$\begin{aligned} v_{\text{eff}}(r) &= \frac{1}{2\pi^2 r} \int_0^\infty k \hat{v}_{\text{eff}}(k) \sin(kr) dk \\ &= \frac{18Z^2 e^2}{\epsilon \pi a^4 r} \int_0^\infty \frac{1}{k^3 (k^2 + \kappa^2)} \left( \cos(ka) - \frac{\sin(ka)}{ka} \right)^2 \sin(kr) dk. \end{aligned}$$

One may solve this integral by expansion of the trigonometric functions, partial fraction decomposition, and, finally, integration by parts in a similar way as for the microion density profile  $\bar{\varrho}_c$ . However, the calculation, although being quite straight forward, is very lengthy and the result is already known (cf. [Den03]). However, we can also derive this result as a limit of the more general theory on layered-shell particles from Chapter 5.

Hence, we have for  $r \leq 2a$

$$\begin{aligned}
 v_{\text{eff}}(r) = v_{\text{mm}}(r) & - \frac{9Z^2e^2}{2\epsilon\kappa^4a^4r} \left\{ \left( 1 - e^{-\kappa r} + \frac{1}{2}\kappa^2r^2 + \frac{1}{24}\kappa^4r^4 \right) \cdot \left( 1 - \frac{1}{\kappa^2a^2} \right) + \frac{2}{\kappa a} e^{-2\kappa a} \sinh(\kappa r) \right. \\
 & + \left[ e^{-2\kappa a} \sinh(\kappa r) + 2\kappa^2ar + \frac{1}{3}\kappa^4(4a^3r + ar^3) \right] \cdot \left( 1 + \frac{1}{\kappa^2a^2} \right) \\
 & \left. - \frac{2r}{a} \left( 1 + 2\kappa^2a^2 + \frac{8}{15}\kappa^4a^4 \right) - \frac{r^3}{3a^3} \left( \kappa^2a^2 + \frac{4}{3}\kappa^4a^4 \right) - \frac{1}{720} \frac{\kappa^4}{a^2} r^6 \right\}
 \end{aligned}$$

and for  $r > 2a$

$$v_{\text{eff}}(r) = \frac{9Z^2e^2}{\epsilon\kappa^4a^4} \left[ \cosh(\kappa a) - \frac{\sinh(\kappa a)}{\kappa a} \right]^2 \frac{e^{-\kappa r}}{r}.$$



## 5. Interaction in multilayered-shell microgels

Before actually studying the case of core-shell microgels, let us consider a more general situation: Suppose we have a macroion consisting of a spherically symmetric charge distribution with  $n$  layers of piecewise constant charge densities  $\tilde{q}_i$  (which can be positive, negative or even zero), where for  $i > 1$  each layer is a spherical shell of width  $d_i = a_i - a_{i-1}$ . Here the  $a_i$  denote the radii of the spheres bounding the shells. In the case  $i = 1$  we write the innermost domain just as a spherical core of charge density  $\tilde{q}_1$  with radius  $a_1$ .

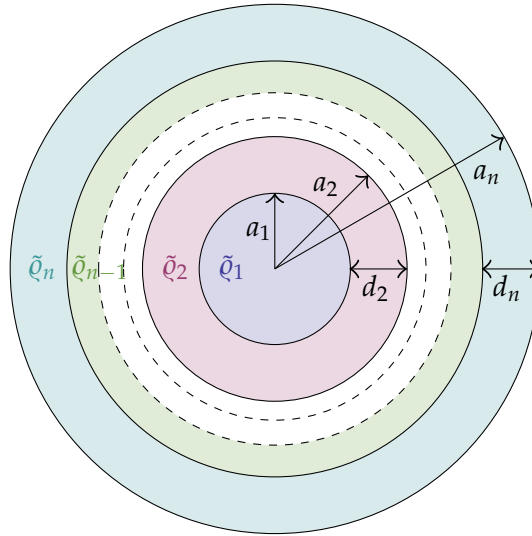


Figure 5.1: Multilayered-shell macroion

Representing each layer by a difference of Heaviside-Functions we obtain the charge distribution

$$\begin{aligned}
 \varrho(\mathbf{x}) &= \sum_{i=2}^n \tilde{q}_i [\Theta(a_i - |\mathbf{x}|) - \Theta(a_{i-1} - |\mathbf{x}|)] + \tilde{q}_1 \Theta(a_1 - |\mathbf{x}|) \\
 &= \tilde{q}_n \Theta(a_n - |\mathbf{x}|) + \sum_{i=1}^{n-1} (\tilde{q}_i - \tilde{q}_{i+1}) \Theta(a_i - |\mathbf{x}|).
 \end{aligned} \tag{5.1}$$

We define  $q_n = \tilde{q}_n$  and  $q_i = \tilde{q}_i - \tilde{q}_{i+1}$  for  $1 \leq i < n$ , so the charge distribution function more conveniently reads

$$q(x) = \sum_{i=1}^n q_i \Theta(a_i - |x|). \quad (5.2)$$

### 5.1. Interaction of multilayered macroions

Considering, as in the previous chapter, a medium of permittivity  $\varepsilon > 0$ , we obtain for the pair interaction between two such macroions separated by a distance  $\mathbf{r}$  the expression

$$\begin{aligned} v_{\text{mm}}(\mathbf{r}) &= \frac{1}{\varepsilon} \int_{\mathbb{R}^6} \frac{q(\mathbf{x})q(\mathbf{y} - \mathbf{r})}{|\mathbf{x} - \mathbf{y}|} d^3x d^3y \\ &= \frac{1}{\varepsilon} \sum_{i,j=1}^n q_i q_j \int_{\mathbb{R}^6} \frac{\Theta(a_i - |\mathbf{x}|)\Theta(a_j - |\mathbf{y} - \mathbf{r}|)}{|\mathbf{x} - \mathbf{y}|} d^3x d^3y. \end{aligned}$$

We define

$$\begin{aligned} \Phi_{ij}(\mathbf{r}) &:= \int_{\mathbb{R}^6} \frac{\Theta(a_i - |\mathbf{x}|)\Theta(a_j - |\mathbf{y} - \mathbf{r}|)}{|\mathbf{x} - \mathbf{y}|} d^3x d^3y \\ &= \int_{\mathbb{R}^3} \Phi_i(\mathbf{y})\Theta(a_j - |\mathbf{y} - \mathbf{r}|) d^3y \end{aligned}$$

with

$$\Phi_i(\mathbf{y}) = \int_{\mathbb{R}^3} \frac{\Theta(a_i - |\mathbf{x}|)}{|\mathbf{x} - \mathbf{y}|} d^3x.$$

Then it follows that

$$v_{\text{mm}}(\mathbf{r}) = \frac{1}{\varepsilon} \sum_{i,j=1}^n q_i q_j \Phi_{ij}.$$

To evaluate the  $x$ -integration, we follow the calculation in Section 4.1 and obtain by Equation (4.3) with  $a \mapsto a_i$

$$\Phi_i(y) = \frac{4\pi a_i^2}{3} \begin{cases} \frac{3}{2} - \frac{1}{2} \frac{y^2}{a_i^2} & \text{for } 0 \leq y \leq a_i. \\ \frac{a_i}{y} & \text{for } y > a_i, \end{cases} \quad (5.3a)$$

$$(5.3b)$$

In the next step we evaluate the remaining integral, which is essentially – i.e. up to a constant factor – the pair interaction between two charged spheres of radii  $a_i$  and  $a_j$ ,

$$\begin{aligned}\Phi_{ij}(\mathbf{r}) &= \int_{\mathbb{R}^3} \Phi_i(\mathbf{y}) \Theta(a_j - |\mathbf{y} - \mathbf{r}|) d^3y \\ &= \int_{\mathbb{R}^3} \Phi_i(|\mathbf{z} + \mathbf{r}|) \Theta(a_j - |\mathbf{z}|) d^3z.\end{aligned}$$

The function  $\Phi_{ij}$  is actually only dependent on the centre-centre separation of the spheres and in spherical coordinates, where the  $\varphi$ -integration has already been performed, reads

$$\Phi_{ij}(r) = 2\pi \int_0^{a_j} \int_0^\pi \Phi_i(|\mathbf{z} + \mathbf{r}|) z^2 \sin \vartheta d\vartheta dz.$$

We start with the case  $r \geq a_i + a_j$ , thus the distance  $|\mathbf{z} + \mathbf{r}| > a_i$  for  $\mathbf{z} \in B_{a_j}(0)$  and  $\Phi_i(|\mathbf{z} + \mathbf{r}|) = \frac{4\pi a_i^2}{3} \frac{a_i}{y}$ . This corresponds to the case, where the two charged spheres are completely separated from each other. Choosing  $\mathbf{r}$  parallel to the  $z$ -axis and substituting  $u := -\cos \vartheta$ , we obtain

$$\begin{aligned}\Phi_{ij}(r) &= \frac{8\pi^2 a_i^3}{3} \int_0^{a_j} z^2 \int_{-1}^1 \frac{1}{\sqrt{z^2 + r^2 - 2rzu}} du dz \\ &= \frac{8\pi^2 a_i^3}{3} \int_0^{a_j} z^2 \left( \frac{1}{zr} (|z + r| - |z - r|) \right) dz.\end{aligned}$$

Since  $r \geq a_i + a_j$  and  $z \leq a_j$ , we have  $r - z \geq a_i \geq 0$ , and thus the integration simplifies to

$$\Phi_{ij}(r) = \frac{16\pi^2 a_i^3}{3r} \int_0^{a_j} z^2 dz = \frac{16\pi^2 a_i^3 a_j^3}{9r}.$$

Now for the remaining cases let, without loss of generality, be  $a_i \geq a_j$ . We consider the case  $a_i \leq r < a_i + a_j$ , that means the two spheres start to overlap. Basically, this turns out to be a slight modification of the situation  $a \leq r < 2a$  in Section 4.1.

We set  $\Phi_{ij}(r) = I_1 + I_2 + I_3$ , where the three integrals are as follows. We have

$$I_1 = \frac{8\pi^2 a_i^3}{3} \int_0^{r-a_i} \int_{-1}^1 \frac{1}{\sqrt{z^2 + r^2 - 2rzu}} z^2 du dz.$$

By Equation (4.6c) this yields

$$I_1 = \frac{8\pi^2 a_i^3}{3} \left( 2a_i^2 - \frac{2a_i^3}{3r} - 2a_i r + \frac{2r^2}{3} \right).$$

## 5. Interaction in multilayered-shell microgels

---

For the second integral we have to evaluate

$$I_2 = \frac{8\pi^2 a_i^3}{3} \int_{r-a_i}^{a_j} \int_{-1}^{\frac{z^2+r^2-a_i^2}{2rz}} \frac{1}{\sqrt{z^2+r^2-2rzu}} z^2 du dz.$$

Using Equation (4.7a), we obtain

$$\begin{aligned} I_2 &= \frac{8\pi^2 a_i^3}{3} \int_{r-a_i}^{a_j} \frac{z(r+z-a_i)}{r} dz \\ &= \frac{8\pi^2 a_i^3}{3} \left( \frac{5a_i^3}{6r} - \frac{5a_i^2}{2} - \frac{a_i a_j^2}{2r} + \frac{5a_i r}{2} + \frac{a_j^3}{3r} + \frac{a_j^2}{2} - \frac{5r^2}{6} \right) \end{aligned}$$

For the third integral we start with an expression analogous to Equation (4.8a), thus we have

$$\begin{aligned} I_3 &= \frac{8\pi^2 a_i^3}{3} \int_{r-a_i}^{a_j} \int_{\frac{z^2+r^2-a_i^2}{2rz}}^1 \left( \frac{3}{2a_i} - \frac{1}{2a_i^3} (z^2+r^2-2rzu) \right) z^2 du dz \\ &= \frac{8\pi^2 a_i^3}{3} \int_{r-a_i}^{a_j} \left( \frac{5a_i z}{8r} - \frac{3rz}{4a_i} + \frac{r^3 z}{8a_i^3} + \frac{3z^2}{2a_i} - \frac{r^2 z^2}{2a_i^3} - \frac{3z^3}{4a_i r} + \frac{3rz^3}{4a_i^3} - \frac{z^4}{2a_i^3} + \frac{z^5}{8a_i^3 r} \right) dz \\ &= \frac{8\pi^2 a_i^3}{3} \left( \frac{a_j^6}{48a_i^3 r} - \frac{a_j^5}{10a_i^3} + \frac{3a_j^4 r}{16a_i^3} - \frac{a_j^3 r^2}{6a_i^3} + \frac{a_j^2 r^3}{16a_i^3} - \frac{r^5}{240a_i^3} - \frac{7a_i^3}{48r} \right. \\ &\quad \left. + \frac{2a_i^2}{5} - \frac{3a_j^4}{16a_i r} + \frac{a_j^3}{2a_i} - \frac{3a_j^2 r}{8a_i} + \frac{5a_i a_j^2}{16r} + \frac{r^3}{16a_i} - \frac{5a_i r}{16} \right). \end{aligned}$$

Finally, the pair interaction up to a constant coefficient, which represents the charge densities, reads

$$\begin{aligned} \Phi_{ij}(r) &= \frac{8\pi^2}{3} \left( \frac{a_i^6}{48r} + \frac{a_j^6}{48r} - \frac{a_i^5}{10} - \frac{a_j^5}{10} - \frac{3a_i^4 a_j^2}{16r} - \frac{3a_i^2 a_j^4}{16r} + \frac{3a_i^4 r}{16} + \frac{3a_j^4 r}{16} \right. \\ &\quad \left. + \frac{a_i^3 a_j^3}{3r} + \frac{a_i^3 a_j^2}{2} + \frac{a_i^2 a_j^3}{2} - \frac{a_i^3 r^2}{6} - \frac{a_j^3 r^2}{6} - \frac{3a_i^2 a_j^2 r}{8} + \frac{a_i^2 r^3}{16} + \frac{a_j^2 r^3}{16} - \frac{r^5}{240} \right). \end{aligned}$$

As expected, the expression is symmetric in  $a_i$  and  $a_j$ , and setting  $a_i = a_j = a$  we can retrieve the pair potential for two homogeneously charged spheres as in Equation (4.9). This result can be extended up to the point  $r = a_i - a_j$  similarly to the case  $0 \leq r \leq a$  in Section 4.1. Although the calculation looks slightly different due to a modified partition of the integration domain, the result, however, turns out to be the same.



So the next really interesting case is the one, where the larger sphere fully covers the smaller one, this corresponds to separation distances  $r < a_i - a_j$ . When carrying out the integration for  $\Phi_{ij}$  the angle  $\vartheta$  is not restricted anymore, and thus we obtain

$$\begin{aligned}\Phi_{ij}(r) &= \frac{8\pi^2 a_i^3}{3} \int_0^{a_j} \int_{-1}^1 \left( \frac{3}{2a_i} - \frac{1}{2a_i^3} (z^2 + r^2 - 2rzu) \right) z^2 du dz \\ &= \frac{8\pi^2}{3} \left( a_i^2 a_j^3 - \frac{a_j^5}{5} - \frac{a_j^3 r^2}{3} \right).\end{aligned}$$

It is worth to mention that this term is not symmetric in  $a_i$  and  $a_j$  anymore (it was done under the assumption of  $a_i \geq a_j$ ), the potential, however, is. Suppose  $a_j > a_i$ , then the calculation would give

$$\Phi_{ij}(r) = \frac{8\pi^2}{3} \left( a_j^2 a_i^3 - \frac{a_i^5}{5} - \frac{a_i^3 r^2}{3} \right).$$

Since in the pair interaction both terms are added, the result is again symmetric. Summarized, we have (assumed  $a_i \geq a_j$ )

$$\Phi_{ij}(r) = \frac{8\pi^2}{3} \left\{ \begin{array}{ll} a_i^2 a_j^3 - \frac{a_j^5}{5} - \frac{a_j^3 r^2}{3} & \text{for } 0 \leq r \leq a_i - a_j, \\ \begin{aligned} & \frac{a_i^6}{48r} + \frac{a_j^6}{48r} - \frac{a_i^5}{10} - \frac{a_j^5}{10} \\ & - \frac{3a_i^4 a_j^2}{16r} - \frac{3a_i^2 a_j^4}{16r} + \frac{3a_i^4 r}{16} \\ & + \frac{3a_j^4 r}{16} + \frac{a_i^3 a_j^3}{3r} + \frac{a_i^3 a_j^2}{2} \\ & + \frac{a_i^2 a_j^3}{2} - \frac{a_i^3 r^2}{6} - \frac{a_j^3 r^2}{6} \\ & - \frac{3a_i^2 a_j^2 r}{8} + \frac{a_i^2 r^3}{16} + \frac{a_j^2 r^3}{16} - \frac{r^5}{240} \end{aligned} & \text{for } a_i - a_j \leq r < a_i + a_j, \\ \frac{2a_i^3 a_j^3}{3r} & \text{for } 0 \leq r \leq a_i - a_j. \end{array} \right.$$

Since the layer bounds are numbered increasingly from 1 to  $n$ , the pair interaction between two macroions can be recast as

$$\begin{aligned}v_{\text{mm}}(r) &= \frac{1}{\varepsilon} \sum_{i,j=1}^n q_i q_j \Phi_{ij}(r) \\ &= \frac{1}{\varepsilon} \sum_{i=1}^n q_i^2 \Phi_{ii}(r) + \frac{2}{\varepsilon} \sum_{i=1}^n \sum_{j=1}^{i-1} q_i q_j \Phi_{ij}(r).\end{aligned}$$

## 5.2. Interaction of a layered macroion and a point charge

We model the charge density of the macroion as in the previous section, thus

$$\varrho(\mathbf{x}) = \sum_{i=1}^n q_i \Theta(a_i - |\mathbf{x}|).$$

The Coulomb interaction of such a macroion situated at the origin and a point charge  $q$  separated by a distance  $\mathbf{r}$  in a medium of permittivity  $\varepsilon > 0$  reads

$$\begin{aligned} v_{\text{mc}}(\mathbf{r}) &= \frac{1}{\varepsilon} \int_{\mathbb{R}^6} \frac{\varrho(\mathbf{x}) q \delta(\mathbf{y} - \mathbf{r})}{|\mathbf{x} - \mathbf{y}|} d^3x d^3y \\ &= \frac{q}{\varepsilon} \sum_{i=1}^n q_i \int_{\mathbb{R}^3} \delta(\mathbf{y} - \mathbf{r}) \int_{\mathbb{R}^3} \frac{\Theta(a_i - |\mathbf{x}|)}{|\mathbf{x} - \mathbf{y}|} d^3x d^3y. \end{aligned}$$

We substitute the integral over  $x$  with the expression calculated in Equation (5.3a), evaluate the  $\delta$ -distribution and obtain

$$v_{\text{mc}}(r) = \frac{q}{\varepsilon} \sum_{i=1}^n q_i \Phi_i(r). \quad (5.4)$$

## 5.3. Counterion density and effective interaction

We calculate the counterion density around a single macroion at the coordinate origin as in Equation (4.13)

$$\langle \hat{\varrho}_c(k) \rangle = \chi(k) \hat{v}_{\text{mc}}(k). \quad (5.5)$$

Remember,  $\chi(k) = -\frac{\varepsilon \lambda_B n_c}{e^2 + \varepsilon \lambda_B n_c \hat{v}_{\text{cc}}(k)}$  is the linear response function and  $\hat{v}_{\text{cc}}(k) = \frac{4\pi q^2}{\varepsilon k^2}$  is the Fourier transform of the Coulomb interaction between two counterions of charge  $q$ . Thus, we need the Fourier transform of the macroion-counterion interaction  $v_{\text{mc}}(r)$ . Since the Fourier transform is linear, we immediately obtain from Equation (5.4)

$$\hat{v}_{\text{mc}}(k) = \frac{q}{\varepsilon} \sum_{i=1}^n q_i \hat{\Phi}_i(k). \quad (5.6)$$

Hence, we can treat every summand  $\Phi_i(r)$  as in Section 4.2 and we obtain

$$\hat{\Phi}_i(k) = \frac{-16\pi^2 a_i}{k^4} \left( \cos(ka_i) - \frac{\sin(ka_i)}{ka_i} \right). \quad (5.7)$$

We substitute the last equation into (5.6) and (5.5), so

$$\langle \hat{\varrho}_c(k) \rangle = \frac{4\pi}{q} \sum_{i=1}^n q_i a_i \frac{\kappa^2}{k^2(k^2 + \kappa^2)} \left( \cos(ka_i) - \frac{\sin(ka_i)}{ka_i} \right) \quad (5.8)$$

and apply the inverse Fourier transform. This yields

$$\bar{q}_c(r) = \frac{2\kappa^2}{\pi q r} \sum_{i=1}^n q_i a_i \int_0^\infty \frac{\sin(kr)}{k(k^2 + \kappa^2)} \left( \cos(ka_i) - \frac{\sin(ka_i)}{ka_i} \right) dk,$$

where the integral is exactly the difference of Equations (4.16) and (4.18), and therefore, each summand of the counterion density is, up to the coefficient, as in Equation (4.20) for  $a = a_i$ . Taking this into account, we obtain

$$\begin{aligned} \bar{q}_c(r) = & -\frac{1}{qr} \left[ \sum_{i=m+1}^n q_i a_i \left( \frac{r}{a_i} - \left( 1 + \frac{1}{\kappa a_i} \right) e^{-\kappa a_i} \sinh(\kappa r) \right) \right. \\ & \left. + \sum_{i=1}^m q_i a_i e^{-\kappa r} \left( \cosh(\kappa a_i) - \frac{\sinh(\kappa a_i)}{\kappa a_i} \right) \right], \end{aligned} \quad (5.9)$$

where  $m$  is the natural number such that  $a_m \leq r < a_{m+1}$ , with  $a_0 = 0$ .

We obtain the effective interaction as  $v_{\text{eff}} = v_{\text{ind}} + v_{\text{mm}}$ , where  $\hat{v}_{\text{ind}}(k) = \langle \hat{q}_c(k) \rangle \hat{v}_{\text{mc}}(k)$ . Combining Equations (5.6)–(5.8) yields

$$\hat{v}_{\text{ind}}(k) = -\frac{64\pi^3}{\varepsilon k^6} \frac{\kappa^2}{k^2 + \kappa^2} \sum_{i,j=1}^n q_i q_j a_i a_j \left( \cos(ka_i) - \frac{\sin(ka_i)}{ka_i} \right) \left( \cos(ka_j) - \frac{\sin(ka_j)}{ka_j} \right).$$

We also need the Fourier transform of the macroion pair interaction, which reads

$$\hat{v}_{\text{mm}}(k) = \frac{1}{\varepsilon} \sum_{i=1}^n q_i^2 \hat{\Phi}_{ii}(k) + \frac{2}{\varepsilon} \sum_{i=1}^n \sum_{j=1}^{i-1} q_i q_j \hat{\Phi}_{ij}(k).$$

The function  $\Phi_{ij}(r)$  is defined piecewise on  $[0, a_i - a_j]$ ,  $[a_i - a_j, a_i + a_j]$  and  $[a_i + a_j, \infty[$ , so the Fourier transform splits into the sum of three integrals on these domains. The calculation of these integrals involves repeated application of the integration-by-parts formulas for trigonometric functions. Doing so, we end up with a result similar to Section 4.2,

$$\hat{\Phi}_{ij}(k) = \frac{64\pi^3}{k^6} a_i a_j \left( \cos(ka_i) - \frac{\sin(ka_i)}{ka_i} \right) \left( \cos(ka_j) - \frac{\sin(ka_j)}{ka_j} \right).$$

Since  $\hat{\Phi}_{ij}(k)$  is symmetric in  $i$  and  $j$  again, we can write

$$\hat{v}_{\text{mm}}(k) = \frac{64\pi^3}{\varepsilon k^6} \sum_{i,j=1}^n q_i q_j a_i a_j \left( \cos(ka_i) - \frac{\sin(ka_i)}{ka_i} \right) \left( \cos(ka_j) - \frac{\sin(ka_j)}{ka_j} \right),$$

and therefore,

$$\hat{v}_{\text{eff}}(k) = \frac{64\pi^3}{\varepsilon k^4} \frac{1}{k^2 + \kappa^2} \sum_{i,j=1}^n q_i q_j a_i a_j \left( \cos(ka_i) - \frac{\sin(ka_i)}{ka_i} \right) \left( \cos(ka_j) - \frac{\sin(ka_j)}{ka_j} \right).$$

## 5. Interaction in multilayered-shell microgels

So the remaining task is to apply the inverse Fourier transform to the effective interaction, then

$$v_{\text{eff}}(r) = \frac{32\pi}{\varepsilon r} \sum_{i,j=1}^n q_i q_j a_i a_j I_{ij}.$$

with

$$I_{ij} = \int_0^\infty \frac{1}{k^3(k^2 + \kappa^2)} \left( \cos(ka_i) - \frac{\sin(ka_i)}{ka_i} \right) \left( \cos(ka_j) - \frac{\sin(ka_j)}{ka_j} \right) \sin(kr) dk.$$

We substitute  $x := \frac{\kappa}{k}$  and obtain

$$\begin{aligned} I_{ij} &= \frac{1}{\kappa^4} \int_0^\infty \frac{1}{x^3(1+x^2)} \left( \cos(a_i \kappa x) - \frac{\sin(a_i \kappa x)}{a_i \kappa x} \right) \left( \cos(a_j \kappa x) - \frac{\sin(a_j \kappa x)}{a_j \kappa x} \right) \sin(r \kappa x) dx \\ &= \frac{1}{4\kappa^4} \int_0^\infty \left( -\frac{\sin((a_i - a_j - r)\kappa x)}{a_i a_j \kappa^2 x^5 (x^2 + 1)} + \frac{\sin((a_i + a_j - r)\kappa x)}{a_i a_j \kappa^2 x^5 (x^2 + 1)} \right. \\ &\quad + \frac{\sin((a_i - a_j + r)\kappa x)}{a_i a_j \kappa^2 x^5 (x^2 + 1)} - \frac{\sin((a_i + a_j + r)\kappa x)}{a_i a_j \kappa^2 x^5 (x^2 + 1)} - \frac{\cos((a_i - a_j - r)\kappa x)}{a_i \kappa x^4 (x^2 + 1)} \\ &\quad + \frac{\cos((a_i - a_j - r)\kappa x)}{a_j \kappa x^4 (x^2 + 1)} - \frac{\cos((a_i + a_j - r)\kappa x)}{a_i \kappa x^4 (x^2 + 1)} - \frac{\cos((a_i + a_j - r)\kappa x)}{a_j \kappa x^4 (x^2 + 1)} \\ &\quad + \frac{\cos((a_i - a_j + r)\kappa x)}{a_i \kappa x^4 (x^2 + 1)} - \frac{\cos((a_i - a_j + r)\kappa x)}{a_j \kappa x^4 (x^2 + 1)} + \frac{\cos((a_i + a_j + r)\kappa x)}{a_i \kappa x^4 (x^2 + 1)} \\ &\quad + \frac{\cos((a_i + a_j + r)\kappa x)}{a_j \kappa x^4 (x^2 + 1)} - \frac{\sin((a_i - a_j - r)\kappa x)}{x^3 (x^2 + 1)} - \frac{\sin((a_i + a_j - r)\kappa x)}{x^3 (x^2 + 1)} \\ &\quad \left. + \frac{\sin((a_i - a_j + r)\kappa x)}{x^3 (x^2 + 1)} + \frac{\sin((a_i + a_j + r)\kappa x)}{x^3 (x^2 + 1)} \right) dx. \end{aligned} \quad (5.10)$$

By decomposing the integrand of  $I_{ij}$  into partial fractions, we obtain terms that can be integrated by parts in a similar way as in Section 4.2. We exclude this part of the calculation since it is too lengthy to be included in detail and just give the final result for  $I_{ij}$  here. Further details on this calculation can be found in Appendix A. The expression actually splits into three cases. At first let  $0 \leq r < a_i - a_j$ , then

$$\begin{aligned} I_{ij} &= \frac{\pi}{12a_i a_j \kappa^6} \left[ 2a_j^3 \kappa^4 r - 3(a_i \kappa + 1)(a_j \kappa - 1)e^{\kappa(-a_i + a_j)} \sinh(\kappa r) \right. \\ &\quad \left. - 3(a_i \kappa + 1)(a_j \kappa + 1)e^{\kappa(-a_i - a_j)} \sinh(\kappa r) \right]. \end{aligned} \quad (5.11)$$

For the case  $a_i - a_j \leq r < a_i + a_j$ , we obtain

$$I_{ij} = \frac{\pi}{96a_i a_j \kappa^6} \left[ -3a_i^4 \kappa^4 + 8a_i^3 \kappa^4 r + 6a_i^2 \kappa^2 (a_j^2 \kappa^2 - \kappa^2 r^2 - 2) - 3a_j^4 \kappa^4 + 8a_j^3 \kappa^4 r \right. \\ \left. - 6a_j^2 \kappa^2 (\kappa^2 r^2 + 2) + \kappa^4 r^4 + 12\kappa^2 r^2 + 24 + 12(a_i \kappa + 1)(a_j \kappa - 1)e^{\kappa(-a_i + a_j - r)} \right. \\ \left. + 12(a_i \kappa - 1)(a_j \kappa + 1)e^{\kappa(a_i - a_j - r)} - 24(a_i \kappa + 1)(a_j \kappa + 1)e^{\kappa(-a_i - a_j)} \sinh(\kappa r) \right]. \quad (5.12)$$

For  $a_i + a_j \leq r$ , we have

$$I_{ij} = \frac{\pi}{2\kappa^4} e^{-\kappa r} \left( \cosh(a_i \kappa) - \frac{\sinh(a_i \kappa)}{a_i \kappa} \right) \left( \cosh(a_j \kappa) - \frac{\sinh(a_j \kappa)}{a_j \kappa} \right). \quad (5.13)$$



## 6. Application to core-shell microgels

This chapter is dedicated to the evaluation of the effective interaction and the counterion density profile for model core-shell macroions. In the setting of Chapter 5 this corresponds to a value of  $n = 2$ , such that a macroion of radius  $a_2 = a$  has a core given as a fraction  $\alpha a$  with  $\alpha \in ]0, 1[$  of the macroion radius  $a$  and a shell of width  $d_2 = (1 - \alpha)a$ . We choose  $Z \geq 0$  to be the charge of the macroion, which is shared between the core and the shell, such that  $Z_2 = \zeta Z$  and  $Z_1 = (1 - \zeta)Z$ , where we have  $\zeta \in ]\infty, \infty[$ .

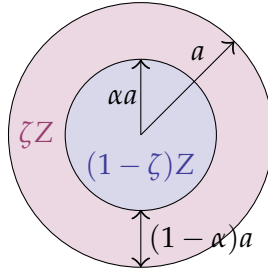


Figure 6.1: Core-shell macroion

Therefore, the charge density of the macroion by Equation (5.2) reads

$$\varrho(x) = \frac{3Ze\zeta}{4\pi a^3(1 - \alpha^3)}\Theta(a_2 - |x|) + \frac{3Ze(\alpha^3 + \zeta - 1)}{4\pi a^3\alpha^3(\alpha^3 - 1)}\Theta(a_1 - |x|)$$

with

$$q_1 = \frac{3Ze(\alpha^3 + \zeta - 1)}{4\pi a^3\alpha^3(\alpha^3 - 1)} \text{ and } q_2 = \frac{3Ze\zeta}{4\pi a^3(1 - \alpha^3)}. \quad (6.1)$$

For the graphical representation we choose a macroion to have net valence  $Z = 3$ , and the counterions shall be negatively monovalent. We measure the distance from the macroion's centre in units of  $a$ . We plot the effective energy  $v_{\text{eff}}$  in units of  $\frac{Z^2 e^2}{\epsilon a}$  and the counterion density profile  $\bar{\varrho}_c$  in units of  $\frac{3Z}{4\pi a^3}$ . We consider several cases with different charges of core and shell of the macroions: At first, we choose macroions with negatively charged core and positively charged shell, then hollow macroions where all the (positive) charge is concentrated within the shell, and finally, macroions where the both core and shell are positively charged but the core carries the higher charge.

## 6. Application to core-shell microgels

- Let  $\zeta = \frac{4}{3}$ , this equals  $Z_2 = 4$  and  $Z_1 = -1$ .

In the first plot (Figure 6.2) we see the effective pair interaction between two macroions for different core fractions  $\alpha$ , setting  $\kappa = \frac{1}{2}$ . We observe a strong dependence on the negative charge density within the core, subject to the electrostatic attraction between the oppositely charged cores and shells of the two macroions. Anyway, we shall see that this effect, even though intuitively expected, may quantitatively be incorrect, due to the negative counterion density in the core region. We will explore this situation in more detail below, see Figure 6.3.

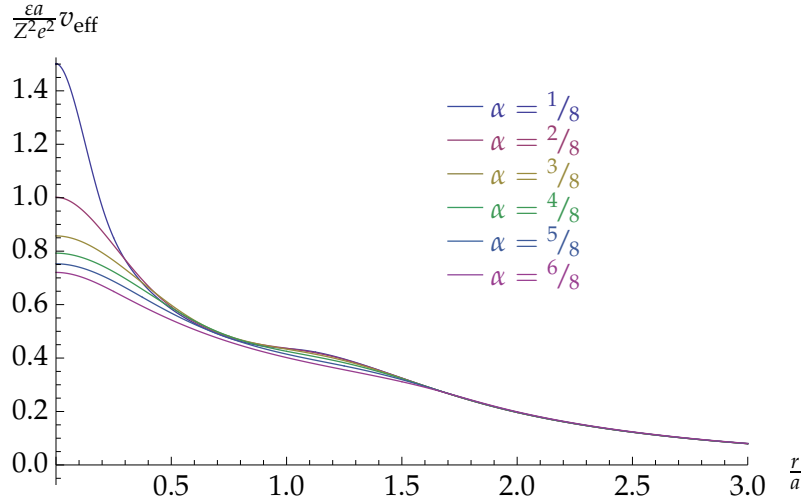


Figure 6.2: Effective interaction, variable  $\alpha$ , constant  $\kappa = \frac{1}{2}$ ,  $\zeta = \frac{4}{3}$

Now we illustrate the counterion density profile around a single macroion for the same situation as above. We find that qualitatively the counterion density profile fits our expectation. However, a closer look at Figure 6.3 shows that the result is of limited reliability as we observe unphysically negative values near the macroion centre for small cores.



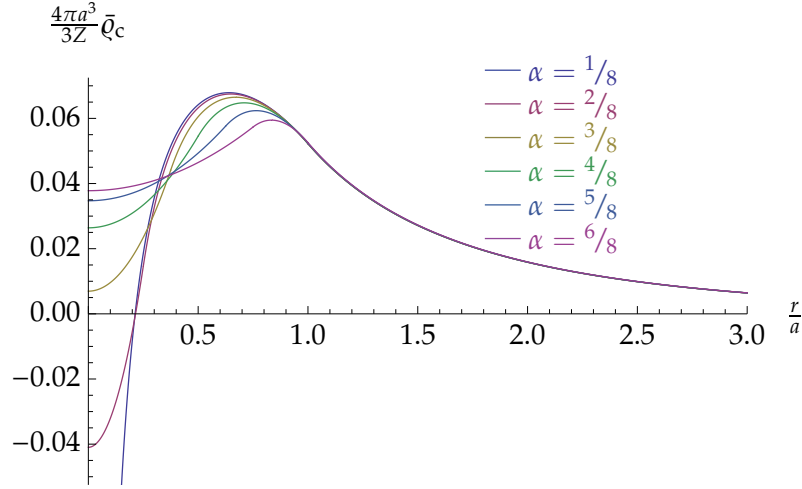


Figure 6.3: Counterion density profile, variable  $\alpha$ , constant  $\kappa = \frac{1}{2}$ ,  $\zeta = \frac{4}{3}$

This (analytical) behaviour is purely subject to the approximation method used and needs considerable more attention. Suitable methods for further exploration include e. g. either computer simulations, higher order perturbation theory, and/or an alternative approach such as the use of integral equations. It should be mentioned that there exists the possibility that for large negative charge densities within the core a perturbative ansatz may even be impossible due to the strong interaction.

The next three plots, Figures 6.4, 6.5, and 6.6, cover the dependence on the screening constant  $\kappa$ . At first, we compare the effective pair interaction with the one for a homogenous particle of the same over-all charge and radius, as well as with the bare macroion pair interaction, which corresponds to the high-temperature limit  $\kappa \rightarrow 0$ . Recall that the relation between the screening constant and the temperature is given by

$$\kappa^2 = \frac{4\pi n_c z^2 e^2}{\epsilon k_B T}.$$

We observe that a lower screening  $\kappa$  corresponds either to a higher temperature  $T$ , to a higher permittivity  $\epsilon$  or to a lower average counterion density  $n_c$ . Since the latter is fixed by the charge neutrality condition  $n_m Z + n_c z = 0$  and the permittivity  $\epsilon$  is given by the electrolyte used, we consider  $\kappa$  to be mainly dependent on the temperature.

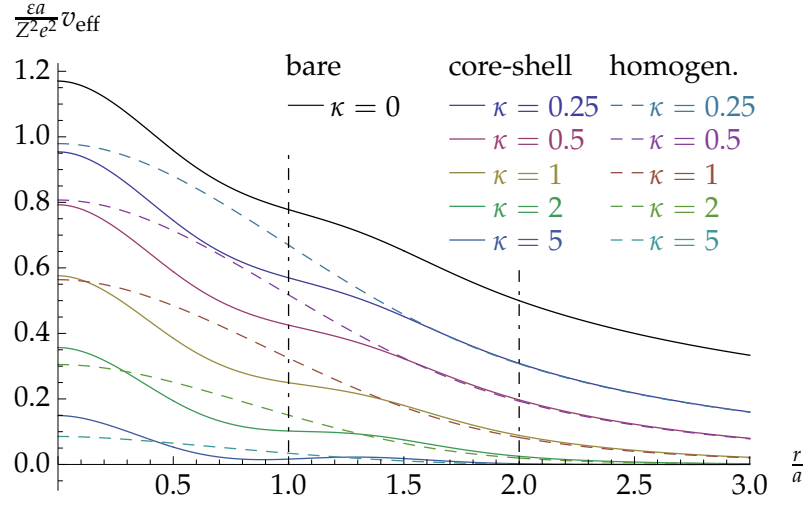


Figure 6.4: Effective interaction, variable  $\kappa$ , constant  $\alpha = \frac{1}{2}$ ,  $\zeta = \frac{4}{3}$

Looking at the counterion density profile (Figure 6.5), we observe a similar unphysical behaviour for large values of the screening constant  $\kappa$  as in the case of a small core.

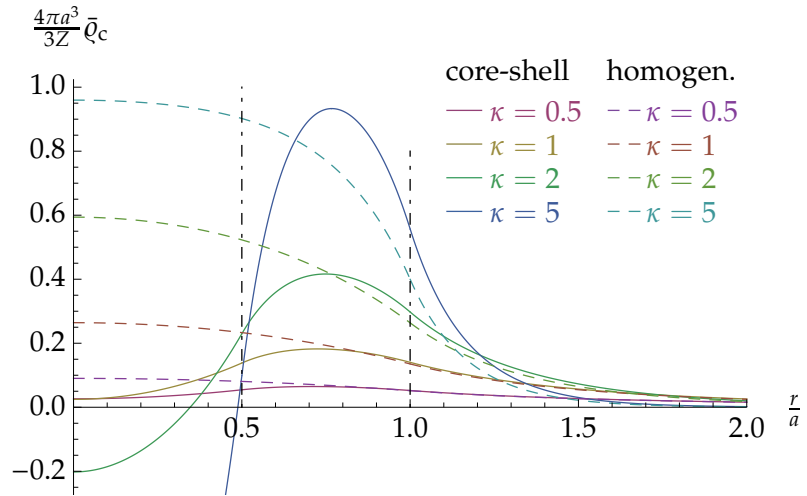


Figure 6.5: Counterion density profile, variable  $\kappa$ , constant  $\alpha = \frac{1}{2}$ ,  $\zeta = \frac{4}{3}$

Finally, to confirm the Yukawa-like behaviour for large radii, in Figure 6.6, we give a semi-logarithmic plot of  $\frac{\epsilon r}{Z^2 e^2} v_{\text{eff}}$ . As expected from Equation (5.13) these graphs are straight lines as in the well-known theory for homogeneous macroions, cf. [Den03].

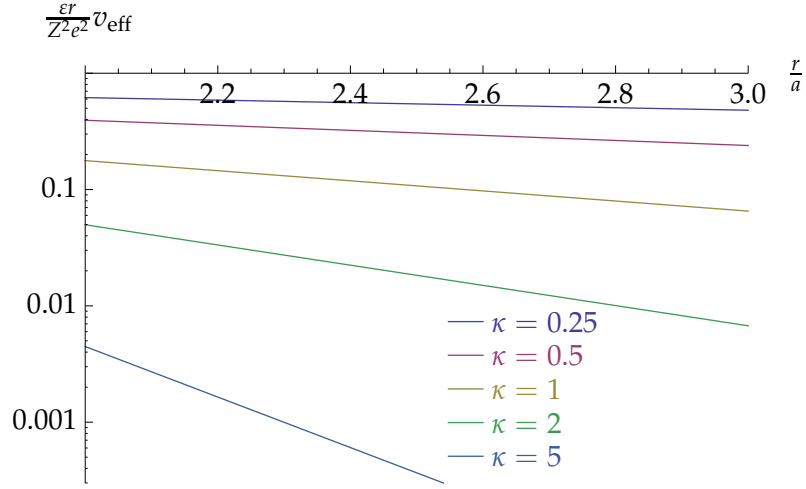


Figure 6.6: Logarithmic plot of the effective interaction, variable  $\kappa$ , constant  $\alpha = \frac{1}{2}$ ,  $\zeta = \frac{4}{3}$

- Let  $\zeta = 1$ , this equals  $Z_2 = 3$  and  $Z_1 = 0$ .

In Figure 6.7, we plot the effective pair interaction for different values of the core radius at constant screening  $\kappa = \frac{1}{2}$ . For distances from the macroion's centre larger than  $2a$  the interaction follows a Yukawa-like fall-off that is nearly independent of the macroion's internal configuration.

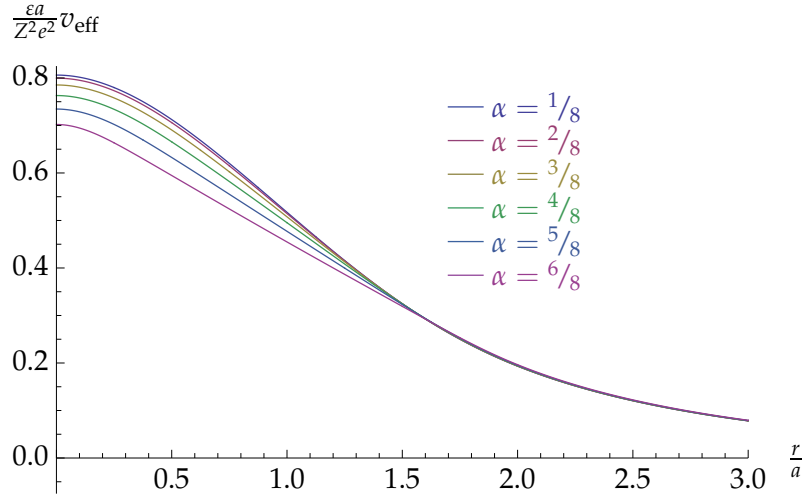


Figure 6.7: Effective interaction, variable  $\alpha$ , constant  $\kappa = \frac{1}{2}$ ,  $\zeta = 1$

Additionally, Figure 6.8 shows the matching counterion density profile. Here, as

expected, the counterion density reaches its maximum near the boundary between core and shell and slightly drops below this value within the neutral core.

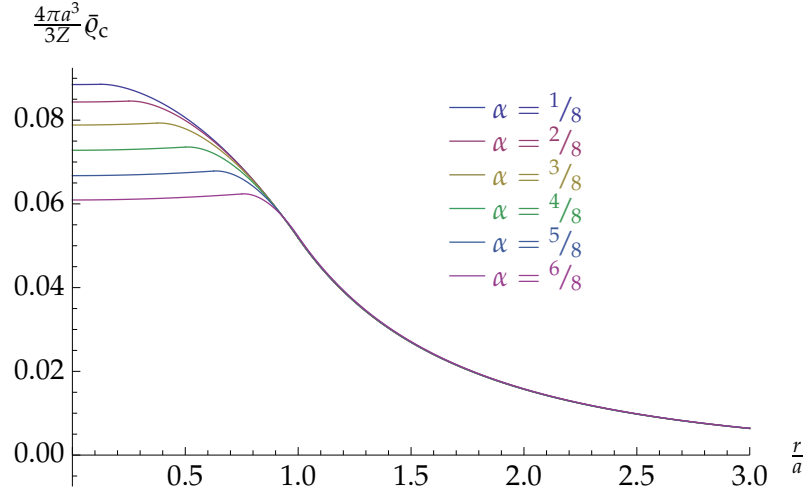


Figure 6.8: Counterion density profile, variable  $\alpha$ , constant  $\kappa = \frac{1}{2}$ ,  $\zeta = 1$

Now, we leave the core radius fraction at a constant value of  $\alpha = \frac{1}{2}$  and instead consider a variable screening  $\kappa$ . The next two plots, Figures 6.9 and 6.10, show the effective interaction and the counterion density profile. We also compare the effective interaction to the one for a homogeneous macroion of same radius and over-all charge.

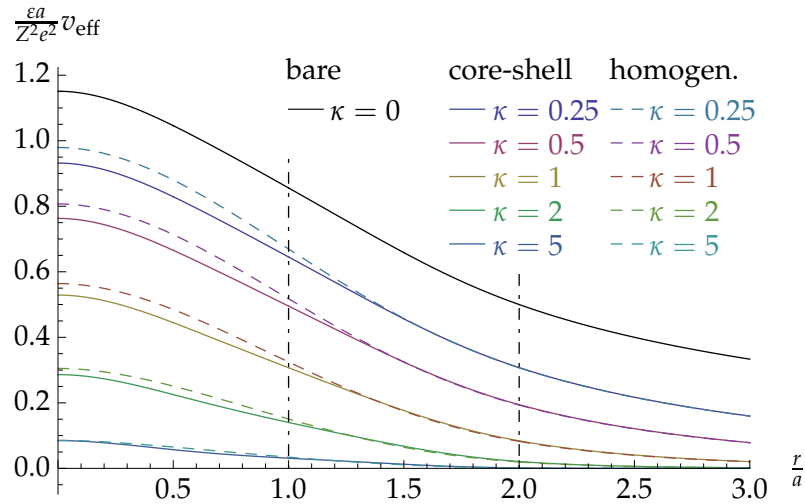


Figure 6.9: Effective interaction, variable  $\kappa$ , constant  $\alpha = \frac{1}{2}$ ,  $\zeta = 1$

Here, we also find that for large radii the theory for core-shell particles approximately matches the case of homogeneous particles. If the shell of one macroion overlaps with the core of the other, the effective repulsion is slightly weaker than compared to the situation with homogeneous macroions since the macroions' cores are neutral.

The counterion density profile shows the expected behaviour for a neutral core particle. The counterion density is maximal within the shell of the particle and decreases within the core, the effect being stronger for a larger screening constant  $\kappa$  and nearly non-existent in the case of weak screening, as the thermal energy of the counterions dominates over the electrostatic interaction. In the limit  $\kappa \rightarrow \infty$ , i. e. we let the temperature approach absolute zero, the counterion density profile converges to a step function, such that all counterions are trapped within the shell of the macroion (actually this situation is not shown in the plot).

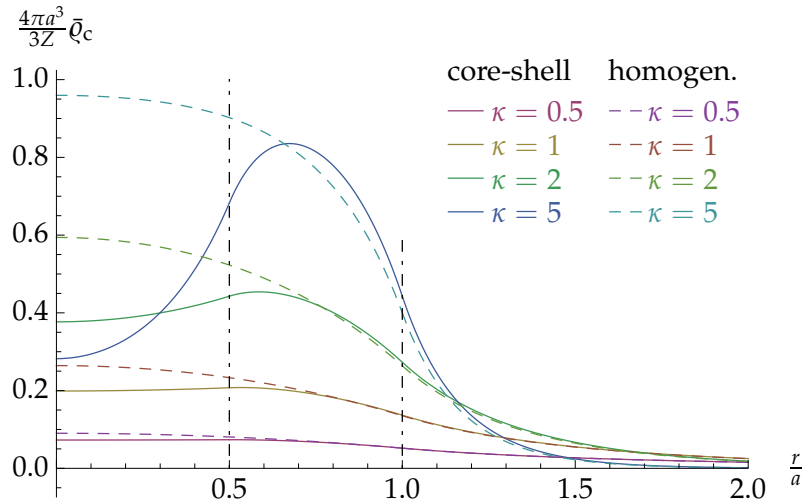


Figure 6.10: Counterion density profile, variable  $\kappa$ , constant  $\alpha = \frac{1}{2}$ ,  $\zeta = 1$

In contrast to the case with a negatively charged core, the linear response approximation in this case gives reasonable results for the counterion density profile, even within the macroion's core.

Again, to illustrate the Yukawa fall-off for large distances, we include a logarithmic plot of  $\frac{\epsilon r}{Z^2 e^2} v_{\text{eff}}(\frac{r}{a})$  which according to Equation (5.13) are straight lines.

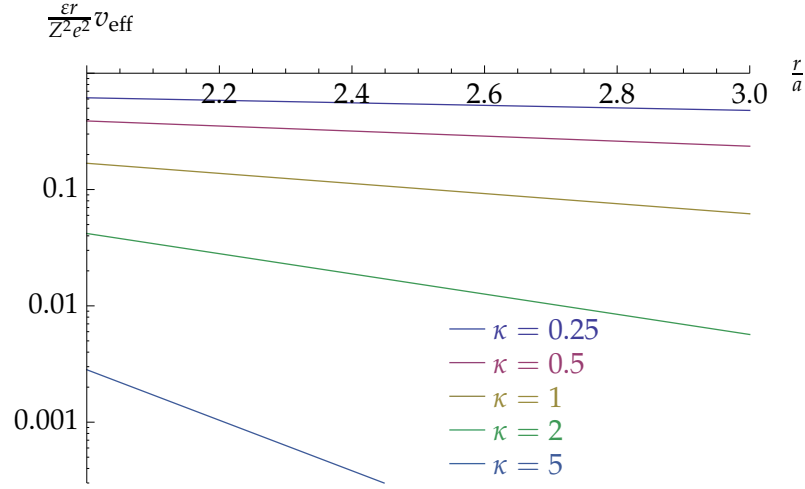


Figure 6.11: Logarithmic plot of the effective interaction, variable  $\kappa$ , constant  $\alpha = \frac{1}{2}$ ,  $\zeta = 1$

- Let  $\zeta = \frac{1}{3}$ , this equals  $Z_2 = 1$  and  $Z_1 = 2$ .

The last case, we consider, is the case of a core shell particle that consists of a positively charged core as well as a positively charged shell as an approximation of a macroion with gradually decreasing charge for increasing distance to the centre. We observe that the effective interaction for small macroion separations is subject to a strong effect as the charge density within the core increases. Here, we choose again  $\kappa = \frac{1}{2}$ .

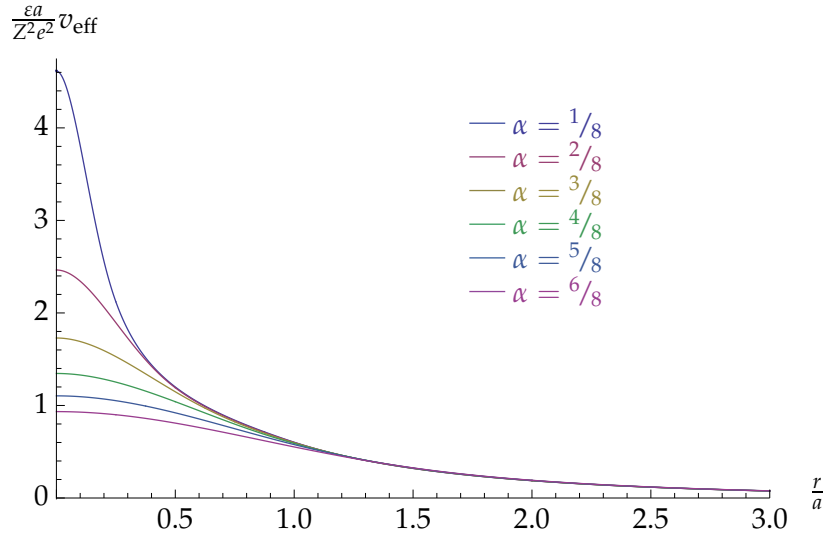


Figure 6.12: Effective interaction, variable  $\alpha$ , constant  $\kappa = \frac{1}{2}$ ,  $\zeta = \frac{1}{3}$

A similar effect can be observed for the counterion density profile: A higher charge density within the core draws a large fraction of the counterions into the core.

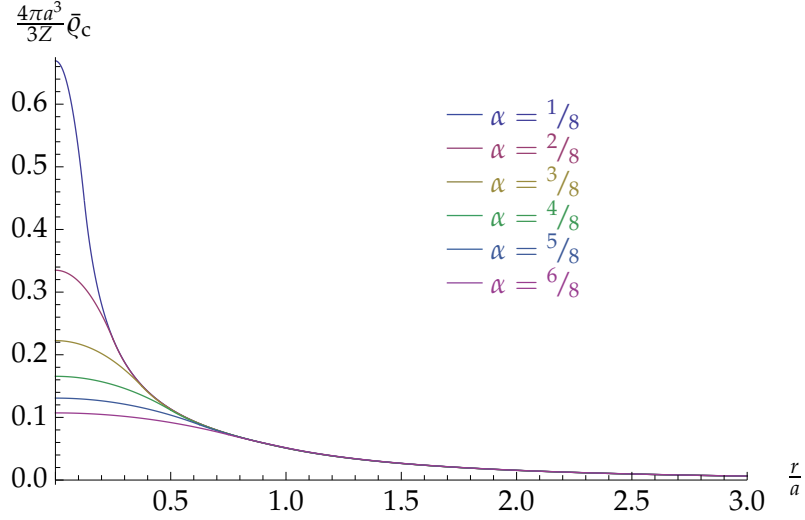


Figure 6.13: Counterion density profile, variable  $\alpha$ , constant  $\kappa = \frac{1}{2}$ ,  $\zeta = \frac{1}{3}$

Now, we set  $\alpha = \frac{1}{2}$  and vary the screening  $\kappa$ . A plot of the effective interaction for a core-shell microgel and one consisting of homogeneous macroions also shows a stronger repulsive potential for core-shell macroions compared to the homogenous case, cf. Figure 6.14.

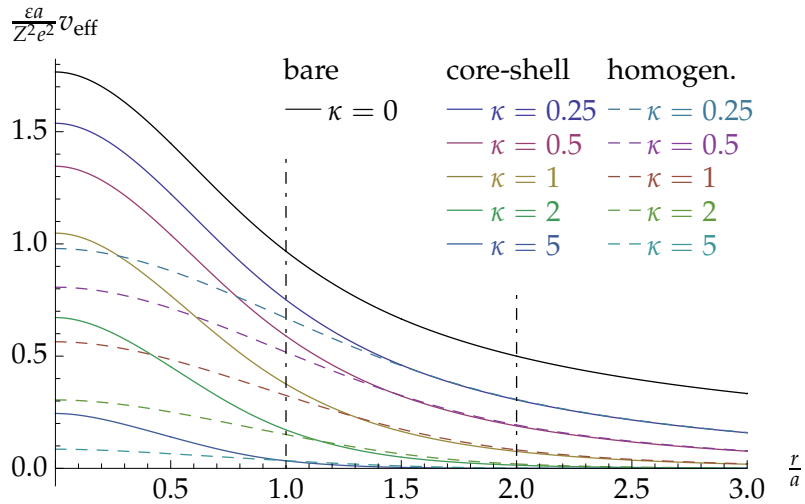


Figure 6.14: Effective interaction, variable  $\kappa$ , constant  $\alpha = \frac{1}{2}$ ,  $\zeta = \frac{1}{3}$

## 6. Application to core-shell microgels

Similarly, the counterion density is significantly higher than in the case of homogeneous macroions, see Figure 6.15.

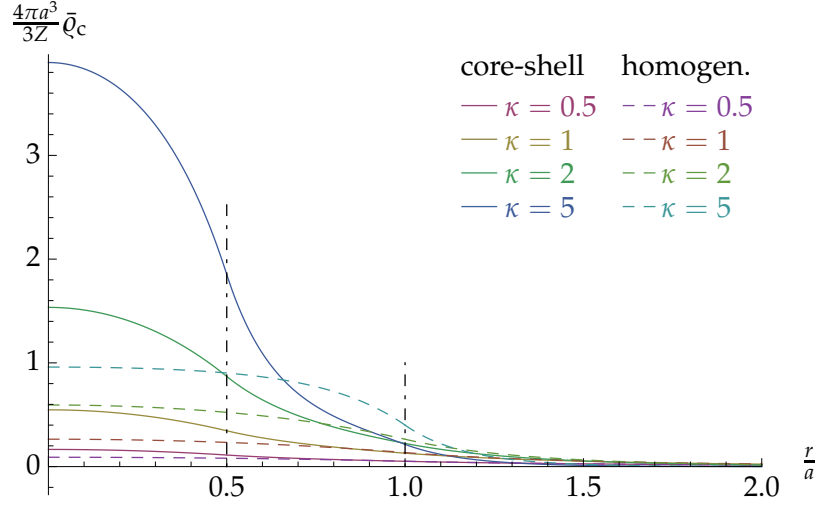


Figure 6.15: Counterion density profile, variable  $\kappa$ , constant  $\alpha = \frac{1}{2}, \zeta = \frac{1}{3}$

The logarithmic plot of the effective interaction illustrates the Yukawa fall-off for large radii. This situation is shown in Figure 6.16.

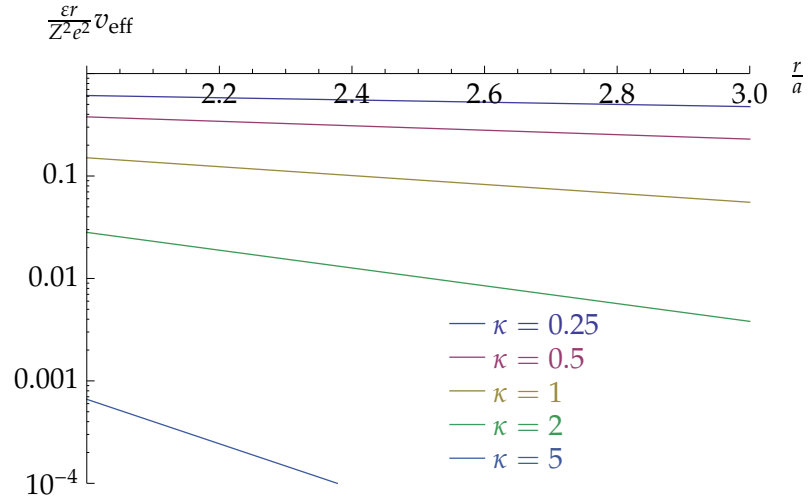


Figure 6.16: Logarithmic plot of the effective interaction, variable  $\kappa$ , constant  $\alpha = \frac{1}{2}, \zeta = \frac{1}{3}$



## A. Fourier integral evaluation

Here, we evaluate the inverse Fourier integral from Equation (5.10). To simplify the following calculations, we split the integrand of (5.10) into a sum of three terms, i.e.  $I_{ij} = A_{ij} + B_{ij} + C_{ij}$  and define the following auxillary constants:

$$\begin{aligned}\alpha &:= (a_i - a_j - r)\kappa & \beta &:= (a_i + a_j - r)\kappa \\ \gamma &:= (a_i - a_j + r)\kappa & \delta &:= (a_i + a_j + r)\kappa\end{aligned}$$

For the first term we obtain

$$\begin{aligned}A_{ij} &= \frac{1}{4\kappa^4} \int_0^\infty \left( -\frac{\sin(\alpha x)}{a_i a_j \kappa^2 x^5} + \frac{\sin(\beta x)}{a_i a_j \kappa^2 x^5} + \frac{\sin(\gamma x)}{a_i a_j \kappa^2 x^5} - \frac{\sin(\delta x)}{a_i a_j \kappa^2 x^5} \right. \\ &\quad + \frac{\sin(\alpha x)}{a_i a_j \kappa^2 x^3} - \frac{\sin(\beta x)}{a_i a_j \kappa^2 x^3} - \frac{\sin(\gamma x)}{a_i a_j \kappa^2 x^3} + \frac{\sin(\delta x)}{a_i a_j \kappa^2 x^3} \\ &\quad - \frac{\cos(\alpha x)}{a_i \kappa x^4} - \frac{\cos(\beta x)}{a_i \kappa x^4} + \frac{\cos(\gamma x)}{a_i \kappa x^4} + \frac{\cos(\delta x)}{a_i \kappa x^4} \\ &\quad + \frac{\cos(\alpha x)}{a_j \kappa x^4} - \frac{\cos(\beta x)}{a_j \kappa x^4} - \frac{\cos(\gamma x)}{a_j \kappa x^4} + \frac{\cos(\delta x)}{a_j \kappa x^4} \\ &\quad \left. - \frac{\sin(\alpha x)}{x^3} - \frac{\sin(\beta x)}{x^3} + \frac{\sin(\gamma x)}{x^3} + \frac{\sin(\delta x)}{x^3} \right) dx \\ &= \frac{1}{4\kappa^4} \lim_{t \rightarrow \infty} \\ &\quad \left( \frac{\alpha \cos(\alpha x)}{2x} - \frac{\alpha^2 \cos(\alpha x)}{6a_i x \kappa} + \frac{\alpha^2 \cos(\alpha x)}{6a_j x \kappa} + \frac{\cos(\alpha x)}{3a_i x^3 \kappa} - \frac{\cos(\alpha x)}{3a_j x^3 \kappa} - \frac{\alpha^3 \cos(\alpha x)}{24a_i a_j x \kappa^2} \right. \\ &\quad - \frac{\alpha \cos(\alpha x)}{2a_i a_j x \kappa^2} + \frac{\alpha \cos(\alpha x)}{12a_i a_j x^3 \kappa^2} \\ &\quad + \frac{\beta \cos(\beta x)}{2x} - \frac{\beta^2 \cos(\beta x)}{6a_i x \kappa} - \frac{\beta^2 \cos(\beta x)}{6a_j x \kappa} + \frac{\cos(\beta x)}{3a_i x^3 \kappa} + \frac{\cos(\beta x)}{3a_j x^3 \kappa} + \frac{\beta^3 \cos(\beta x)}{24a_i a_j x \kappa^2} \\ &\quad \left. + \frac{\beta \cos(\beta x)}{2a_i a_j x \kappa^2} - \frac{\beta \cos(\beta x)}{12a_i a_j x^3 \kappa^2} \right)\end{aligned}$$

### A. Fourier integral evaluation

$$\begin{aligned}
& -\frac{\gamma \cos(\gamma x)}{2x} + \frac{\gamma^2 \cos(\gamma x)}{6a_i x \kappa} - \frac{\gamma^2 \cos(\gamma x)}{6a_j x \kappa} - \frac{\cos(\gamma x)}{3a_i x^3 \kappa} + \frac{\cos(\gamma x)}{3a_j x^3 \kappa} + \frac{\gamma^3 \cos(\gamma x)}{24a_i a_j x \kappa^2} \\
& + \frac{\gamma \cos(\gamma x)}{2a_i a_j x \kappa^2} - \frac{\gamma \cos(\gamma x)}{12a_i a_j x^3 \kappa^2} \\
& - \frac{\delta \cos(\delta x)}{2x} + \frac{\delta^2 \cos(\delta x)}{6a_i x \kappa} + \frac{\delta^2 \cos(\delta x)}{6a_j x \kappa} - \frac{\cos(\delta x)}{3a_i x^3 \kappa} - \frac{\cos(\delta x)}{3a_j x^3 \kappa} - \frac{\delta^3 \cos(\delta x)}{24a_i a_j x \kappa^2} \\
& - \frac{\delta \cos(\delta x)}{2a_i a_j x \kappa^2} + \frac{\delta \cos(\delta x)}{12a_i a_j x^3 \kappa^2} \\
& - \frac{\alpha \sin(\alpha x)}{6a_i x^2 \kappa} + \frac{\alpha \sin(\alpha x)}{6a_j x^2 \kappa} + \frac{\sin(\alpha x)}{2x^2} - \frac{\alpha^2 \sin(\alpha x)}{24a_i a_j x^2 \kappa^2} - \frac{\sin(\alpha x)}{2a_i a_j x^2 \kappa^2} + \frac{\sin(\alpha x)}{4a_i a_j x^4 \kappa^2} \\
& - \frac{\beta \sin(\beta x)}{6a_i x^2 \kappa} - \frac{\beta \sin(\beta x)}{6a_j x^2 \kappa} + \frac{\sin(\beta x)}{2x^2} + \frac{\beta^2 \sin(\beta x)}{24a_i a_j x^2 \kappa^2} + \frac{\sin(\beta x)}{2a_i a_j x^2 \kappa^2} - \frac{\sin(\beta x)}{4a_i a_j x^4 \kappa^2} \\
& + \frac{\gamma \sin(\gamma x)}{6a_i x^2 \kappa} - \frac{\gamma \sin(\gamma x)}{6a_j x^2 \kappa} - \frac{\sin(\gamma x)}{2x^2} + \frac{\gamma^2 \sin(\gamma x)}{24a_i a_j x^2 \kappa^2} + \frac{\sin(\gamma x)}{2a_i a_j x^2 \kappa^2} - \frac{\sin(\gamma x)}{4a_i a_j x^4 \kappa^2} \\
& + \frac{\delta \sin(\delta x)}{6a_i x^2 \kappa} + \frac{\delta \sin(\delta x)}{6a_j x^2 \kappa} - \frac{\sin(\delta x)}{2x^2} - \frac{\delta^2 \sin(\delta x)}{24a_i a_j x^2 \kappa^2} - \frac{\sin(\delta x)}{2a_i a_j x^2 \kappa^2} + \frac{\sin(\delta x)}{4a_i a_j x^4 \kappa^2} \Bigg) \Bigg|_{x=0}^t \\
& + \frac{1}{4\kappa^4} \lim_{t \rightarrow \infty} \left( -\frac{\alpha^4 \text{Si}(\alpha x)}{24a_i a_j \kappa^2} - \frac{\alpha^2 \text{Si}(\alpha x)}{2a_i a_j \kappa^2} + \frac{\beta^4 \text{Si}(\beta x)}{24a_i a_j \kappa^2} + \frac{\beta^2 \text{Si}(\beta x)}{2a_i a_j \kappa^2} \right. \\
& + \frac{\gamma^4 \text{Si}(\gamma x)}{24a_i a_j \kappa^2} + \frac{\gamma^2 \text{Si}(\gamma x)}{2a_i a_j \kappa^2} - \frac{\delta^4 \text{Si}(\delta x)}{24a_i a_j \kappa^2} - \frac{\delta^2 \text{Si}(\delta x)}{2a_i a_j \kappa^2} \\
& - \frac{\alpha^3 \text{Si}(\alpha x)}{6a_i \kappa} - \frac{\beta^3 \text{Si}(\beta x)}{6a_i \kappa} + \frac{\gamma^3 \text{Si}(\gamma x)}{6a_i \kappa} + \frac{\delta^3 \text{Si}(\delta x)}{6a_i \kappa} \\
& + \frac{\alpha^3 \text{Si}(\alpha x)}{6a_j \kappa} - \frac{\beta^3 \text{Si}(\beta x)}{6a_j \kappa} - \frac{\gamma^3 \text{Si}(\gamma x)}{6a_j \kappa} + \frac{\delta^3 \text{Si}(\delta x)}{6a_j \kappa} \\
& \left. + \frac{1}{2} \alpha^2 \text{Si}(\alpha x) + \frac{1}{2} \beta^2 \text{Si}(\beta x) - \frac{1}{2} \gamma^2 \text{Si}(\gamma x) - \frac{1}{2} \delta^2 \text{Si}(\delta x) \right) \Bigg|_{x=0}^t
\end{aligned}$$

Obviously, the first part of  $A_{ij}$ , containing only sine and cosine functions converges to zero for  $t \rightarrow \infty$ . To obtain the value for  $x = 0$ , we expand these terms into a Taylor series and observe that the constant term vanishes. More precisely, the series expansion reads

$$-\frac{4}{3}(a_i^2 \kappa^3 r + a_j^2 \kappa^3 r - 6\kappa r)x + \mathcal{O}(x^3).$$

Since  $\text{Si}(0) = 0$ , the terms consisting of sine integrals can be evaluated as

$$\lim_{x \rightarrow \infty} \text{Si}(\lambda x) = \frac{\pi}{2} \text{sgn } \lambda. \quad (\text{A.1})$$

We now turn to  $B_{ij}$ , which reads

$$\begin{aligned}
B_{ij} = & \frac{1}{4\kappa^4} \int_0^\infty \left( \frac{x \sin(\alpha x)}{a_i a_j \kappa^2 (x^2 + 1)} - \frac{x \sin(\beta x)}{a_i a_j \kappa^2 (x^2 + 1)} - \frac{x \sin(\gamma x)}{a_i a_j \kappa^2 (x^2 + 1)} + \frac{x \sin(\delta x)}{a_i a_j \kappa^2 (x^2 + 1)} \right. \\
& - \frac{\sin(\alpha x)}{a_i a_j \kappa^2 x} + \frac{\sin(\beta x)}{a_i a_j \kappa^2 x} + \frac{\sin(\gamma x)}{a_i a_j \kappa^2 x} - \frac{\sin(\delta x)}{a_i a_j \kappa^2 x} \\
& - \frac{\cos(\alpha x)}{a_i \kappa (x^2 + 1)} - \frac{\cos(\beta x)}{a_i \kappa (x^2 + 1)} + \frac{\cos(\gamma x)}{a_i \kappa (x^2 + 1)} + \frac{\cos(\delta x)}{a_i \kappa (x^2 + 1)} \\
& + \frac{\cos(\alpha x)}{a_j \kappa (x^2 + 1)} - \frac{\cos(\beta x)}{a_j \kappa (x^2 + 1)} - \frac{\cos(\gamma x)}{a_j \kappa (x^2 + 1)} + \frac{\cos(\delta x)}{a_j \kappa (x^2 + 1)} \\
& - \frac{x \sin(\alpha x)}{x^2 + 1} - \frac{x \sin(\beta x)}{x^2 + 1} + \frac{x \sin(\gamma x)}{x^2 + 1} + \frac{x \sin(\delta x)}{x^2 + 1} \\
& \left. + \frac{\sin(\alpha x)}{x} + \frac{\sin(\beta x)}{x} - \frac{\sin(\gamma x)}{x} - \frac{\sin(\delta x)}{x} \right) dx.
\end{aligned}$$

We can easily evaluate this expression using (A.1), thus

$$\int_0^\infty \frac{\cos(\lambda x)}{1 + x^2} dx = \frac{\pi}{2} e^{-|\lambda|} \text{ and } \int_0^\infty \frac{x \sin(\lambda x)}{1 + x^2} dx = \frac{\pi}{2} e^{-|\lambda|} \operatorname{sgn} \lambda.$$

Finally, for the third expression we obtain

$$\begin{aligned}
C_{ij} = & \frac{1}{\kappa^4} \int_0^\infty \left( \frac{\cos(\alpha x)}{a_i \kappa x^2} + \frac{\cos(\beta x)}{a_i \kappa x^2} - \frac{\cos(\gamma x)}{a_i \kappa x^2} - \frac{\cos(\delta x)}{a_i \kappa x^2} \right. \\
& \left. - \frac{\cos(\alpha x)}{a_j \kappa x^2} + \frac{\cos(\beta x)}{a_j \kappa x^2} + \frac{\cos(\gamma x)}{a_j \kappa x^2} - \frac{\cos(\delta x)}{a_j \kappa x^2} \right) dx \\
= & \frac{1}{4\kappa^4} \lim_{t \rightarrow 0} \left( -\frac{\cos(\alpha x)}{a_i \kappa x} - \frac{\cos(\beta x)}{a_i \kappa x} + \frac{\cos(\gamma x)}{a_i \kappa x} + \frac{\cos(\delta x)}{a_i \kappa x} \right. \\
& \left. + \frac{\cos(\alpha x)}{a_j \kappa x} - \frac{\cos(\beta x)}{a_j \kappa x} - \frac{\cos(\gamma x)}{a_j \kappa x} + \frac{\cos(\delta x)}{a_j \kappa x} \right) \Big|_{x=0}^t \\
& + \frac{1}{4\kappa^4} \lim_{t \rightarrow 0} \left( -\frac{\alpha \operatorname{Si}(\alpha x)}{a_i \kappa} - \frac{\beta \operatorname{Si}(\beta x)}{a_i \kappa} + \frac{\gamma \operatorname{Si}(\gamma x)}{a_i \kappa} + \frac{\delta \operatorname{Si}(\delta x)}{a_i \kappa} \right. \\
& \left. + \frac{\alpha \operatorname{Si}(\alpha x)}{a_j \kappa} - \frac{\beta \operatorname{Si}(\beta x)}{a_j \kappa} - \frac{\gamma \operatorname{Si}(\gamma x)}{a_j \kappa} + \frac{\delta \operatorname{Si}(\delta x)}{a_j \kappa} \right) \Big|_{x=0}^t
\end{aligned}$$

The first part of  $C_{ij}$  converges to zero for  $t \rightarrow \infty$ , similar to  $A_{ij}$ . Again, we expand into a Taylor series to evaluate this expression for  $x = 0$ , this gives

$$-8x(\kappa r) + \mathcal{O}(x^3).$$

For the sine integrals we use again (A.1). Reinserting  $\alpha$ ,  $\beta$ ,  $\gamma$ , and  $\delta$  yields (5.11), (5.12), and (5.13) if we employ a case-by-case analysis for the three cases  $0 \leq r < a_i - a_j$ ,  $a_i - a_j \leq r < a_i + a_j$ , and  $a_i + a_j \leq r$ .



# Index

- background
  - energy, 12
  - uniform compensating, 12
- Bjerrum length, 15
- canonical partition function, 11
- charge
  - density, 14
- charge density
  - core-shell macroion, 45
  - multilayered macroion, 36
- colloid, 1
- counterion, 2
  - density profile, 15
    - homogeneous charge, 27
    - multilayered charge, 41
  - free energy, 12, 15
  - pair interaction, 10
- de Broglie wavelength
  - thermal, 11
- Debye screening length, 15
- density profile
  - counterion, 15
    - homogeneous charge, 27, 31
    - multilayered charge, 41
- dielectric constant, 9, 19
- distribution
  - derivative of a, 4
  - tempered, 3
- distributional derivative, 4
- dominated convergence, 7
- effective
  - Hamiltonian, 16
  - interaction, 2
    - homogeneous charge, 33
    - multilayered charge, 42
- energy
  - background, 12
  - free, 12
  - volume, 17
- Fourier transform, 5
  - evaluation, 55
  - inverse, 5
  - radial, 6
- free energy
  - counterion, 12, 15
  - of a one-component plasma, 14
- gel, 1
  - micro, 1
- Hamiltonian
  - effective, 16
  - of a microgel, 10
- induced interaction, 16
  - homogeneous charge, 31

- multilayered charge, 41
- integrable regulator, 6
- integral equations, 47
- interaction
  - Coulomb, 10
  - effective, 2
    - homogeneous charge, 33
    - multilayered charge, 42
  - induced, 16
    - homogeneous charge, 31
    - multilayered charge, 41
  - pair
    - homogeneous charge, 19
    - multilayered charge, 36, 39
- length
  - Bjerrum, 15
  - Debye, 15
- linear response
  - approximation, 13
  - function, 15
- macroion, 2
  - multilayered, 35
  - pair interaction, 10, 25
- macroion-counterion
  - pair interaction, 11, 25
  - multilayered charge, 40
- microgel, 1
  - Hamiltonian, 10
  - solution, 9
- multilayered
  - macroion, 35
  - shell
    - microgel, 35
- one-component
  - plasma
    - classical, 13
- free energy, 14
  - reduction, 10
- pair interaction
  - counterion, 10
  - homogeneous charge, 19
  - macroion, 10, 25
  - macroion-counterion, 11, 25
  - multilayered charge, 36, 39
- partition function
  - canonical, 11
- permittivity
  - electric, 9, 19
- perurbation theory
  - higher order, 47
  - second order, 13
- plasma
  - one-component, 13
    - free energy, 14
- pseudoparticles, 2
- reduction
  - one-component, 10
- regulator
  - integrable, 6
- Schwartz space, 3
- static structure factor, 15
- structure factor
  - static, 15
- suspension
  - colloidal, 1
- tempered distribution, 3
- thermal de Broglie wavelength, 11
- volume energy, 17







## References

- [ARF13] G. AGUIRRE, J. RAMOS, and J. FORCADA: *Synthesis of new enzymatically degradable thermo-responsive nanogels*. *Soft Matter*, **9**:261–270, 2013. [2](#)
- [AsSt78] N. W. ASHCROFT and D. STROUD: *Theory of the thermodynamics of simple liquid metals*. volume 33 of *Solid State Physics*, 1–81, Academic Press, 1978. [12](#)
- [Bak49] W. O. BAKER: *Microgel, a new macromolecule*. *Industrial & Engineering Chemistry*, **41**(3):511–520, 1949. [1](#)
- [BRV05] M. BRADLEY, J. RAMOS, and B. VINCENT: *Equilibrium and kinetic aspects of the uptake of poly(ethylene oxide) by copolymer microgel particles of n-isopropylacrylamide and acrylic acid*. *Langmuir*, **21**(4):1209–1215, 2005. [2](#)
- [BTH03] L. BROMBERG, M. TEMCHENKO, and T. A. HATTON: *Smart microgel studies. polyelectrolyte and drug-absorbing properties of microgels from polyether-modified poly(acrylic acid)*. *Langmuir*, **19**(21):8675–8684, 2003. [1](#)
- [Den99] A. R. DENTON: *Effective interactions and volume energies in charge-stabilized colloidal suspensions*. *Journal of Physics: Condensed Matter*, **11**(50):10061–10071, 1999. [2](#), [10](#)
- [Den00] A. R. DENTON: *Effective interactions and volume energies in charged colloids: Linear response theory*. *Phys. Rev. E*, **62**:3855–3864, 2000. [10](#)
- [Den03] A. R. DENTON: *Counterion penetration and effective interactions in solutions of polyelectrolyte stars and microgels*. *Physical Review E*, **67**:011804–011813, 2003. [2](#), [10](#), [15](#), [32](#), [48](#)
- [FPLC07] X. FENG, R. PELTON, M. LEDUC, and S. CHAMP: *Colloidal complexes from poly(vinyl amine) and carboxymethyl cellulose mixtures*. *Langmuir*, **23**(6):2970–2976, 2007. [1](#)
- [Fri98] F. G. FRIEDLANDER: *Introduction to the theory of distributions*. Cambridge University Press, Cambridge, second edition, 1998, with additional material by M. Joshi. [3](#), [4](#)

## References

---

- [FuSa49] R. FUOSS and H. SADEK: *Mutual interaction of polyelectrolytes*. Science, **110**(2865):552–554, 1949. [1](#)
- [GSK05] Z. GUO, H. SAUTEREAU, and D. E. KRANBUEHL: *Structural evolution and heterogeneities studied by frequency-dependent dielectric sensing in a styrene/dimethacrylate network*. Macromolecules, **38**(19):7992–7999, 2005. [1](#)
- [HaMc06] J.-P. HANSEN and I. R. McDONALD: *Theory of simple liquids*. Academic Press, London, third edition, 2006. [9](#), [15](#)
- [ImFo11] A. IMAZ and J. FORCADA: *Synthesis strategies to incorporate acrylic acid into n-vinylcaprolactam-based microgels*. Journal of Polymer Science Part A: Polymer Chemistry, **49**(14):3218–3227, 2011. [2](#)
- [JeGu02] B. JEONG and A. GUTOWSKA: *Lessons from nature: stimuli-responsive polymers and their biomedical applications*. Trends in Biotechnology, **20**(7):305–311, 2002. [1](#)
- [CHS05] V. Castro LOPEZ, J. HADGRAFT, and M. J. SNOWDEN: *The use of colloidal microgels as a (trans)dermal drug delivery system*. International Journal of Pharmaceutics, **292**(1–2):137–147, 2005. [1](#)
- [LSea04] L. A. LYON, J. D. DEBORD, S. B. DEBORD, C. D. JONES, J. G. MCGRATH, and M. J. SERPE: *Microgel colloidal crystals*. The Journal of Physical Chemistry B, **108**(50):19099–19108, 2004. [1](#)
- [Mic65] A. S. MICHAELS: *Polyelectrolyte complexes*. Industrial & Engineering Chemistry, **57**(10):32–40, 1965. [1](#)
- [MuSn95] M. J. MURRAY and M. J. SNOWDEN: *The preparation, characterisation and applications of colloidal microgels*. Advances in Colloid and Interface Science, **54**(0):73–91, 1995. [1](#)
- [MFea03] N. MURTHY, M. XU, S. SCHUCK, J. KUNISAWA, N. SHASTRI, and J. M. J. FRÉCHET: *A macromolecular delivery vehicle for protein-based vaccines: Acid-degradable protein-loaded microgels*. Proceedings of the National Academy of Sciences, **100**(9):4995–5000, 2003. [1](#)
- [RLL03] J. R. RETAMA, B. LOPEZ-RUIZ, and E. LOPEZ-CABARCOS: *Microstructural modifications induced by the entrapped glucose oxidase in cross-linked polyacrylamide microgels used as glucose sensors*. Biomaterials, **24**(17):2965–2973, 2003. [1](#)
- [SaVi99] B. R. SAUNDERS and B. VINCENT: *Microgel particles as model colloids: theory, properties and applications*. Advances in Colloid and Interface Science, **80**(1):1–25, 1999. [1](#)

- [Sch45] Laurent SCHWARTZ: *Généralisation de la notion de fonction, de dérivation, de transformation de Fourier et applications mathématiques et physiques*. Ann. Univ. Grenoble. Sect. Sci. Math. Phys. (N.S.), **21**:57–74 (1946), 1945. [3](#)
- [SeRi99] H. SENFF and W. RICHTERING: *Temperature sensitive microgel suspensions: Colloidal phase behavior and rheology of soft spheres*. The Journal of Chemical Physics, **111**(4):1705–1711, 1999. [1](#)
- [XKea03] S. XU, J. ZHANG, C. PAQUET, Y. LIN, and E. KUMACHEVA: *From hybrid microgels to photonic crystals*. Advanced Functional Materials, **13**(6):468–472, 2003. [1](#)



# Curriculum Vitae

---

## Personal data

**Name:** Clemens Gregor Hanel  
**Nationality:** Austrian

---

## School

**09/1986-06/1990:** Volksschule Scheibenbergstraße, 1180 Wien  
**09/1990-06/1998:** Bundesgymnasium Kloostergasse, 1180 Wien  
**06/1998:** School leaving examination

---

## University

**03/1999–11/2006:** Diploma curriculum in mathematics at the University of Vienna  
Master thesis: *Linear hyperbolic second order partial differential equations on spacetime*  
**10/1999–07/2013:** Diploma/Bachelor curriculum in physics at the University of Vienna  
**since 07/2013:** Master curriculum in physics at the University of Vienna  
Master thesis: *Effective interaction in microgels*  
**11/2006–12/2011:** Doctoral curriculum in natural sciences at the Faculty of Mathematics, University of Vienna  
Dissertation: *On singular wave equations*

## Distinctions and grants

06/1998:	School leaving examination with distinction
06/2001:	1 <sup>st</sup> diploma examination in mathematics with distinction
06/2002:	1 <sup>st</sup> diploma examination in physics with distinction
2002:	Scholarship for excellent studies in physics
04/2005–11/2006:	Sponsored master thesis at the Faculty of Mathematics, University of Vienna (FWF-Project Y-237, <i>Nonlinear Distributional Geometry</i> )
11/2006:	2 <sup>nd</sup> diploma examination in mathematics with distinction
02/2011–10/2011:	Research grant of the University of Vienna
12/2011:	Thesis defence with distinction
01/2013:	2 <sup>nd</sup> diploma examination in physics with distinction
07/2013:	Bachelor of Science awarded with distinction

---

## Stays abroad

10/2002–02/2003:	Erasmus grant at the Freie Universität Berlin
------------------	---

---

## Employment history

03/1999–03/2000:	Employee of Wr. Allianz Leasing GmbH & Co. KG, 1010 Wien (part time)
01/2000–01/2005:	System administrator for Amalthea Verlag, 1030 Wien (part time)
since 01/2002:	System administrator for the general practitioner Monika Burkart (MD), 1170 Wien (part time)
12/2006–09/2009:	Research assistant at the Faculty of Mathematics, University of Vienna (full time)
07/2009–03/2010:	Consulting editor (mathematics) for Manz Schulbuch Verlag (part time)
since 09/2009:	Teaching fellow at the University of Vienna (part time)
10/2009–01/2011:	System administrator at the University of Vienna (full time)

---

## Academic activities

### Publications

- Clemens Hanel. *Linear hyperbolic second order partial differential equations on space time*. Master thesis, University of Vienna, Nov. 2006.
- Clemens Hanel. *On singular wave equations*. Dissertation, University of Vienna, Dec. 2011.
- Clemens Hanel, Eberhard Mayerhofer, Stevan Pilipović and Hans Vernaeve. *Homogeneity in generalized function algebras*. J. Math. Anal. Appl., 399(2):899–904, 2008.
- Clemens Hanel. *Wave-type equations of low regularity*. Appl. Anal., 90(11):1691–1705, 2011.
- Clemens Hanel, Günther Hörmann, Christian Spreitzer and Roland Steinbauer. *Wave equations and symmetric first-order systems in case of low regularity*. In *Pseudo-Differential Operators, Generalized Functions and Asymptotics*. Operator Theory: Advances and Applications, accepted for publication.

### Conference participation

- International Conference of Generalized Functions 2009 (Vienna), Talk: *Wave equations and singular spacetimes*.
- 8<sup>th</sup> International ISAAC Congress 2011 (Moscow), Talk: *Hyperbolic PDEs in Colombeau algebras*.
- 12<sup>th</sup> British Gravity Meeting 2012 (Southampton), Talk: *Generalized hyperbolicity in the context of nonlinear distributional geometry*.

### Teaching

Laboratory Tutor: *Physics for Nutritional Scientists*  
Department of Material Physics, University of Vienna

**Summer 2005–Winter 2006**

Exercises: *Functional Analysis 1*  
Faculty of Mathematics, University of Vienna

**Winter 2008**

<i>Exercises: Linear algebra for Physicists</i> Faculty of Physics, University of Vienna	<b>Winter 2008, Winter 2010</b>
<i>Exercises: Analysis for Physicists 1</i> Faculty of Physics, University of Vienna	<b>Winter 2009</b>
<i>Exercises: Analysis for Physicists 2</i> Faculty of Physics, University of Vienna	<b>Summer 2010</b>
<i>Exercises: Linear algebra for Economists</i> Faculty of Economics, University of Vienna	<b>Winter 2010</b>
<i>Exercises: Introduction to Business Mathematics</i> Faculty of Economics, University of Vienna	<b>Winter 2011–Winter 2012</b>
<i>Exercises: Probability for Economists</i> Faculty of Economics, University of Vienna	<b>Winter 2011, Winter 2012</b>
<i>Lecture: Business Statistics 1</i> Faculty of Economics, University of Vienna	<b>Summer 2012–Winter 2012</b>

### **Miscellaneous**

- Organizer of the Colloquium for Master and PhD Students at the Faculty of Mathematics, University of Vienna (2007–2011)

---

### **Languages**

- German (native tongue)
- English (fluent)
- French (basic knowledge)



## Zusammenfassung

Wir verwenden den Formalismus der Ein-Komponenten-Reduktion, um die effektive Wechselwirkung und das Dichteprofil der Gegenionen in einem Mikrogel, das aus Makroionen besteht, welche sich aus mehreren geladenen Schichten zusammensetzen. Dabei folgen wir einem Ansatz, der auf Störungstheorie in zweiter Ordnung basiert und erhalten analytische Ausdrücke für die effektive Wechselwirkung, indem wir die Schichten der Makroionen als Linearkombination homogen geladener Kugeln modellieren. Außerdem wenden wir das allgemeine Resultat auf den wichtigen Fall der *Core-Shell*-Mikrogele an und vergleichen die Theorie mit den bekannten Resultaten für homogen geladene kugelförmige Makroionen.